Deuteron NMR of Methyl Groups in the Tunneling Regime. A Single Crystal Study of Aspirin-CD_3

A. Detken, P. Focke, H. Zimmermann, and U. Haeberlen

Max-Planck-Institut für Medizinische Forschung, Jahnstraße 29, 69120 Heidelberg, Germany

Z. Olejniczak and Z. T. Lalowicz

Institute of Nuclear Physics, Radzikowskiego 152, 31-342 Kraków, Poland

Z. Naturforsch. **50 a**, 95–116 (1995); received October 4, 1994

We dedicate this paper to Prof. Dr. Werner Müller-Warmuth on the occasion of his 65th birthday. Z. T. L. and U. H. owe much to his advice.

We report the first single crystal deuteron NMR spectra of CD_3 groups which display the so-called $\pm\beta$, $\pm(|\alpha| \pm \beta)$ and $\pm(2|\alpha| \pm \beta)$ lines characteristic of rotational tunneling in a sufficiently clear manner to allow a quantitative comparison with the respective theory developed in 1988 by the group of W. Müller-Warmuth. The molecular system we study is aspirin-CD_3. We recorded spectra for differently oriented single crystals and measured spin-lattice relaxation times T_1 in a wide temperature range. At 12.5 K we exploit the dependence of the $\pm(|\alpha| \pm \beta)$ and $\pm(2|\alpha| \pm \beta)$ lines on the orientation of the applied field $\boldsymbol{B}_0$ for determining the equilibrium orientation of the CD_3 group in the crystal lattice. The spectra display features which allow, by comparison with simulated spectra, a measurement of the tunnel frequency ν_t. Its low temperature limit is (2.7 ± 0.1) MHz. It allows to infer the height V_3 of the potential $V(\varphi)$ in which the CD_3 group moves, provided that this potential is purely threefold. We get $V_3 = (47.2 \pm 0.5)$ meV. The transition from the tunneling to the classical, fast reorienting regime occurs in the 15 K $\lesssim T \lesssim$ 35 K temperature range. In this range we observe a broadening, merging and eventually narrowing of the $\pm|\alpha|$ and $\pm 2|\alpha|$ lines in very much the way predicted by Heuer. His theory, however, must be extended by taking into account all librational levels. The behaviour of the $\pm\beta$ lines in the transition temperature range signalizes a reduction of the *observable* tunnel frequency with increasing temperature. This reduction allows an independent measurement of the potential height and represents a test of the assumption of a purely threefold potential. From the T_1-data we derive the temperature dependence of the correlation time τ_c of the reorientational jumps. The plot of $\log \tau_c$ vs. $1/T$ follows a straight line for more than five decades. From its slope we get yet another independent number for the potential height. It agrees well with the other ones, which confirms the assumption of the essentially threefold potential $V(\varphi)$ in aspirin-CD_3.

1. Introduction

At room temperature the high field deuteron NMR spectrum of a deuterated methyl group consists of one pair of lines. We assume, naturally, that the CD_3 group is part of a molecule in a molecular crystal. The pair splitting $\Delta\omega_Q$ reflects the interaction of the deuterons' quadrupole moments with the motionally averaged electric field gradients at the sites of the deuterons. The motions in question are rotational jumps of the $-CD_3$ group about the carbon bond which links the group to the rest of the molecule. In this paper we inquire what happens when the temperature T of the crystal is lowered to, say, 10 K.

There are two limiting cases. In the first, the (angular) coordinate φ which describes the reorientations is adequately conceived as a classical stochastic function of time characterized by a jump rate W. When T is lowered, the rate W just slows down and the methyl group eventually becomes immobile in the same sense as a *methylene* group in, say, polyethylene becomes immobile at sufficiently low temperatures. The NMR spectrum then consists of three pairs of lines, one pair from each of the three deuterons of the CD_3 group, and all lines have the same intensity. The deuterated

Reprint requests to Prof. Dr. U. Haeberlen.

0932-0784 / 95 / 0100-0095 $ 06.00 © – Verlag der Zeitschrift für Naturforschung, D-72027 Tübingen

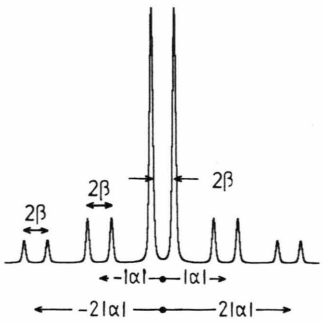

Fig. 1. Prototype deuteron NMR spectrum of a CD_3 group in the tunneling regime when ν_t is very much larger than the quadrupolar coupling constant, which is roughly 160 kHz. The splittings $|\alpha|$ and β are explained in the text, and expressions for them are given in Section 2.

methyl groups in dimethylmalonic acid are an excellent example for this limiting case [1]. At temperatures $T \lesssim 50$ K the methyl groups are immobile in this compound.

However, something else may also happen. Instead of just becoming immobile, the methyl groups may enter into the tunneling regime. In Sect. 2 we shall define carefully what we mean by "tunneling regime". In this regime the coordinate φ must be treated as a quantum mechanical variable. Such a description including the calculation of the deuteron spectrum has been provided in 1988 by Lalowicz, Werner, and Müller-Warmuth [2]. An extra quantity, the tunnel frequency ν_t, also to be defined in Sect. 2, comes into play and affects the deuteron NMR spectrum in a profound way. We stress that the classical case for $W \to 0$ is contained in the quantum mechanical description as the limiting case $\nu_t \to 0$. The prototype spectrum which Lalowicz et al. predicted for the opposite case where the tunnel frequency is very much larger than the deuteron quadrupole coupling constant C_Q (which roughly is 160 kHz) is shown in Figure 1. This spectrum consists of a central pair of lines with a relative intensity of twelve and an inner and an outer pair of pairs of satellites. The inner and outer satellites have relative intensities of two and one, respectively. The displacements of the inner satellite pairs from the Larmor frequency are denoted by $\pm|\alpha|$. The outer satellite pairs are displaced by twice that amount. The *splitting* of all pairs is equal. It is denoted by 2β and is equal to the splitting $\Delta\omega_Q$ of the pair of lines in the high temperature spectrum. The crucial point is that none of the lines in the spectrum of Fig. 1 can be ascribed to a particular deuteron. The spectrum is that of a strongly coupled triple of nuclei. The observation of a spectrum like that in Fig. 1 does not allow to determine the tunnel frequency ν_t. What can be concluded is that the methyl group is in the tunneling regime (which *is* a valuable conclusion) and that ν_t is very much larger than all the quadrupolar frequencies of the system. Hints for CD_3 groups in this regime have been found by Rössler et al. in powder spectra of hexamethylbenzene in various glass matrices [3], [4]. The first single crystal spectra which unambiguously displayed tunneling satellite resonances have been observed by Bernhard et al. from CD_3OH in the inclusion compound hydrochinon [5] and by Manz from methyl-deuterated paraxylene in Dianin's inclusion compound [6]. Because both these inclusion compounds provide "many" different possible sites for their guests (three and six, respectively), the deuteron NMR spectra of these compounds are very complicated and could not be analyzed in great detail.

In the experimental Sect. 3 of this paper we shall present deuteron spectra from single crystals of aspirin-CD_3 which closely resemble that in Fig. 1 and display clearly all the essential features of a CD_3 group in the tunneling regime with ν_t much larger than C_Q.

If the tunnel frequency ν_t is comparable with C_Q, the deuteron spectrum will display features which allow to infer the size of ν_t. As for the exact meaning of "comparable" in this context we refer again to Section 2. For some special orientations of our aspirin-CD_3 crystals we can indeed detect such features. They become more pronounced and eventually observable for all crystal orientations if the temperature is increased to above 23 K. We are thus in a position to measure the temperature dependence of the observable tunnel frequency. Hewson [7] and Würger [8] have discussed such a dependence theoretically in the context of protonated methyl groups and inelastic neutron scattering.

Knowledge of the tunnel frequency ν_t for $T \to 0$ allows to calculate the height of the potential $V(\varphi)$ in which the methyl group moves (if we make certain simplifying assumptions, see Section 2). Another means for learning about this height is measuring the spin lattice relaxation time T_1 and analyzing its temperature dependence [9]. This we have also done. The

number we get in this way for the potential height is in excellent agreement with that derived from the tunnel frequency ν_t, see Section 5.

A theory of how the deuteron spectrum of a CD_3 group in the tunneling regime evolves when the temperature is raised to, eventually, room temperature has been developed by Heuer [10]. Of particular interest is the temperature behaviour of the satellite lines. According to Heuer they should broaden, eventually merge pairwise and sharpen up again in the spectral position of one of the large central lines in exactly the same way as the spectrum of two exchanging, chemically shifted spin-1/2 nuclei behaves when the exchange rate increases. The parameter Γ of the tunneling CD_3 group which is analogous to the exchange rate of the chemically shifted spin-1/2 nuclei is predicted to increase with temperature according to the Arrhenius equation. The corresponding activation energy should be identifiable with the excitation energy to the first librational level of the CD_3 group. Aspirin-CD_3 also offers an excellent opportunity for testing these predictions of Heuer. Our results verify the essential ideas of Heuer's theory but imply that the interpretation of the activation energy must be modified.

In the following Sect. 2 we derive what kinds of deuteron NMR spectra are to be expected from CD_3 groups in the tunneling regime. Our treatment differs from that in [2] in two major aspects: First, we avoid the usual *ad-hoc* introduction of a nonphysical tunneling operator. This will allow us in a natural way to extend the calculation beyond the so-called "pocket-state" approximation [11]. Second, the emphasis will be on single crystal rather than on powder spectra, and we shall specifically consider the regime where the tunnel frequency is comparable with C_Q. This is motivated by the observation of the respective type of spectra in aspirin-CD_3.

2. Theory of deuteron NMR spectra of tunneling CD_3 groups

NMR spectra are usually calculated by diagonalizing a *spin Hamiltonian* $\mathcal{H}_S$ which contains spin components as the only dynamical variables. *Spatial* coordinates may also appear in $\mathcal{H}_S$ but they play the role of *parameters* and, if molecular motions are considered, that of classical functions of time. The calculation of the NMR spectrum of a CH_3 or CD_3 group in the "tunneling regime" (to be defined below) requires, by contrast, the diagonalization of a Hamiltonian $\mathcal{H}$ which contains, in addition to the spin components, at least one spatial coordinate as a dynamical variable. This leads, as we shall see, to a coupling of the spins with dramatic consequences for the NMR spectrum.

2.1 Hamiltonian $\mathcal{H}$ of the methyl group

The Hamiltonian of a CD_3 group in a large magnetic field $\boldsymbol{B}_0$ contains, naturally, a Zeeman, $\mathcal{H}_Z$, a quadrupolar, $\mathcal{H}'_Q$, and a dipolar term, $\mathcal{H}'_D$.

The Zeeman term takes into account the interaction of the deuteron spins with the applied field $\boldsymbol{B}_0 = (0, 0, B_0)$. It depends on the spin components I_z^i of the three deuterons $i = 1, 2, 3$ and is given by

$$\mathcal{H}_Z = -\gamma_D \hbar B_0 \sum_{i=1}^{3} I_z^i. \tag{1}$$

The index "z" refers to the *lab*-frame in which $\boldsymbol{B}_0$ points along the z-axis. Our experiments are carried out in a field B_0 of 11 Tesla, therefore the Larmor frequency $\nu_L := \gamma_D \cdot B_0/(2\pi)$ is 72.1 MHz.

The quadrupole Hamiltonian $\mathcal{H}_Q = \sum_{i=1}^{3} \mathcal{H}_Q^i$ describes the interaction of the quadrupole moment eQ of each deuteron with the electric field gradient (EFG) at its location. This term is responsible for the prominent features of the deuteron NMR spectrum. Its size is characterized by the *quadrupole coupling constant* $C_Q := e^2qQ/h$, where eq is the largest principal component of the EFG tensor. A typical value of C_Q for a deuteron in a methyl group is 160 kHz and is thus very much smaller than ν_L. Therefore we may restrict ourselves to the so-called secular part of $\mathcal{H}_Q$, which is denoted by $\mathcal{H}'_Q$ and given by

$$\mathcal{H}'_Q = \frac{1}{8} h C_Q \sum_{i=1}^{3} (3(I_z^i)^2 - I(I+1))(3\cos^2 \vartheta_i - 1). \tag{2}$$

$I(I+1)$ equals 2 for deuterons; ϑ_i is the angle subtended by the direction of the C–D^i bond and $\boldsymbol{B}_0$. Writing $\mathcal{H}'_Q$ in the form of (2), we have (realistically) assumed that the same quadrupole coupling constant C_Q applies to all three deuterons and that the EFG tensor at the site of each deuteron is axially symmetric with the symmetry axis pointing along the respective C–D bond. We shall return to these assumptions in

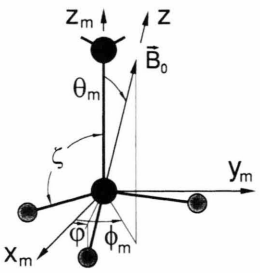

Fig. 2. Orientation of the CD_3 group and of the applied field $\boldsymbol{B}_0$ in the molecular axes system x_m, y_m, z_m.

the experimental section, and shall actually question them.

In Fig. 2 we have drawn a methyl group placed in an axes system x_m, y_m, z_m which we shall call *molecular axes system*. We consider the group as a rigid body, i.e., we neglect all internal vibrations. We assume that it has exact C_3 symmetry and that the C_3-axis has a fixed orientation in space. The methyl group then represents a one-dimensional rotor with the angle φ defined in Fig. 2 as the only dynamical variable. The z_m axis of the molecular axes system is defined as pointing along the C_3-axis of the methyl group, all three hydrogens (deuterons from now on) lie in a plane parallel to the x_m, y_m plane. The direction of the x_m-axis in this plane is arbitrary at this point, we shall dispose of it further down.

Clearly the three angles ϑ_i in (2) are not independent. They all depend on φ and are related by the (assumed) C_3-symmetry of the CD_3 group. In the molecular axes system the polar angles of $\boldsymbol{B}_0$ are denoted by θ_m, ϕ_m. In terms of these angles and the angle ζ subtended by the CD_3 axis and any C–D bond we get

$$\begin{aligned}
\cos\vartheta_1(\varphi) &= \cos\zeta\cos\theta_m \\
&\quad + \sin\zeta\sin\theta_m\cos(\phi_m - \varphi), \\
\cos\vartheta_2(\varphi) &= \cos\zeta\cos\theta_m \\
&\quad + \sin\zeta\sin\theta_m\cos(\phi_m - (\varphi + \tfrac{2\pi}{3})), \\
\cos\vartheta_3(\varphi) &= \cos\zeta\cos\theta_m \\
&\quad + \sin\zeta\sin\theta_m\cos(\phi_m - (\varphi - \tfrac{2\pi}{3})).
\end{aligned} \tag{3}$$

By inserting (3) into (2) we get an expression of $\mathcal{H}'_Q$ which displays explicitly its dependence on the spatial and spin dynamic variables φ and I_z^i. In addition to these *variables*, $\mathcal{H}'_Q$ depends on *parameters* which characterize the CD_3 group (C_Q and ζ) or specify its orientation with respect to the applied field (θ_m and ϕ_m).

The dipolar Hamiltonian $\mathcal{H}'_D$ (truncated with respect to both $\mathcal{H}_Z$ and $\mathcal{H}'_Q$) determines the width of individual resonances in the deuteron NMR spectrum but has no effect upon its prominent features. Therefore we shall contend ourselves here with a few remarks. $\mathcal{H}'_D$ has two parts. The first takes into account the spin-spin interactions of the deuterons within the CD_3 group while the second describes the interactions between the spins of these three deuterons and all other spins in the sample, regardless whether or not they belong to (other) CD_3 groups and regardless of whether or not they are *deuteron* spins. The first part depends again on the dynamic variables φ and I_z^i and can be treated in perfect analogy to $\mathcal{H}'_Q$. In our numerical calculations we include it. The second part constitutes a many-particle problem which we do not (and cannot) treat explicitly. We take it into account as a heuristic lorentzian or gaussian line broadening.

For the following the crucial point is that the spatial coordinate φ appears in $\mathcal{H}'_Q$ (and $\mathcal{H}'_D$). As stated in the Introduction, the usual NMR way of dealing with such a coordinate is to consider it to be a classical stochastic function of time. This viewpoint is insufficient if one observes, as we do, spectra like that in Figure 1. We therefore must treat φ as a quantum mechanical variable. This *forces* us to include in the Hamiltonian $\mathcal{H}$ also the kinetic and potential energy terms connected with φ. The *kinetic* term is $-B\frac{d^2}{d\varphi^2} = -\frac{\hbar^2}{2\Theta}\frac{d^2}{d\varphi^2}$, where B is the rotational constant and Θ the moment of inertia of the CD_3 group. B equals 0.327 meV. The *potential* term is given by the potential $V(\varphi)$ which the methyl group senses when it rotates. This is the place to decide upon the choice of the direction of the x_m-axis: We choose it such that $V(\varphi)$ has a *minimum* for $\varphi = 0$.

The sum of the kinetic and potential energy terms makes up what we are going to call the *rotor Hamiltonian* $\mathcal{H}_R$. The total Hamiltonian is thus

$$\mathcal{H} = \mathcal{H}_R + \mathcal{H}_Z + \mathcal{H}'_Q + \mathcal{H}'_D. \tag{4}$$

For calculating the deuteron NMR spectrum we must diagonalize this Hamiltonian. To this end we must decide upon a set of basis functions. These functions necessarily consist of a space and a spin part. For the space part, which depends on the variable φ, we are going to take the eigenfunctions of $\mathcal{H}_R$. We therefore briefly discuss the rotor Hamiltonian $\mathcal{H}_R$ and its

eigenfunctions. We shall argue, in particular, that we may restrict ourselves to those corresponding to the three lowest eigenvalues.

2.2 *The Mathieu equation and its eigenfunctions* $\Psi(\varphi)$

The Schrödinger equation associated with $\mathcal{H}_R$ reads [12]

$$\mathcal{H}_R\Psi(\varphi) := \left[-\frac{\hbar^2}{2\Theta}\frac{d^2}{d\varphi^2} + V(\varphi)\right]\Psi(\varphi) = E\,\Psi(\varphi). \tag{5}$$

We stated that $V(\varphi)$ has a minimum for $\varphi = 0$ by definition. Due to the assumed C_3 symmetry of the CD_3 group and the indistinguishability of the deuterons the potential $V(\varphi)$ must obey the relation $V(\varphi) = V(\varphi \pm 2\pi/3)$, i.e., it must have two other minima at $\varphi = \pm 2\pi/3$. The simplest form of $V(\varphi)$ satisfying this requirement is

$$V(\varphi) = \frac{1}{2}V_3(1 - \cos 3\varphi), \tag{6}$$

where V_3 is the *height* of the potential. With this expression for $V(\varphi)$, (5) is known as the Mathieu equation. It can be solved numerically. This we have done (as have others), and we shall need some of the results further down. However, it is also instructive to consider some special cases which can be solved analytically, and to discuss the *structure* of the solutions in the general case. One limiting case is the absence of any potential V. The eigenfunctions of $\mathcal{H}_R$ are then the free rotor functions $\frac{1}{\sqrt{2\pi}}\exp(\pm in\varphi)$ with $n = 0, \pm 1, \pm 2, \ldots$ and associated energies $E_n = n^2 B$.

The other limiting case is that where V_3 is virtually infinite. The states $\Psi(\varphi)$ can then be chosen to be localized and for each energy level E_n, called *librational* level n, there are three degenerate states $\Psi_1^{(n)}, \Psi_2^{(n)}, \Psi_3^{(n)}$. The first, say, is localized at $\varphi = 0$ while the second and third are localized at $\varphi = +2\pi/3$ and $\varphi = -2\pi/3$. Instead of taking $\Psi_1^{(n)}$ etc. as solutions of (5) for $V_3 \to \infty$ we may equally well take the linear combinations

$$\begin{aligned} |nA\rangle &= \tfrac{1}{\sqrt{3}}(\Psi_1^{(n)} + \Psi_2^{(n)} + \Psi_3^{(n)}), \\ |nE^a\rangle &= \tfrac{1}{\sqrt{3}}(\Psi_1^{(n)} + \varepsilon\Psi_2^{(n)} + \varepsilon^\star\Psi_3^{(n)}), \\ |nE^b\rangle &= \tfrac{1}{\sqrt{3}}(\Psi_1^{(n)} + \varepsilon^\star\Psi_2^{(n)} + \varepsilon\Psi_3^{(n)}) \end{aligned} \tag{7}$$

with $\varepsilon = \exp(2\pi i/3)$.

The functions on the l.h.s. of (7) are eigenfunctions with eigenvalues $p = 1, \varepsilon$ and $\varepsilon^\star$ of the generator $\mathcal{P}_m$ of *even* permutations of the masses of the three deuterons of the CD_3 group, i.e., $\mathcal{P}_m|nA\rangle = |nA\rangle; \mathcal{P}_m|nE^a\rangle = \varepsilon|nE^a\rangle; \mathcal{P}_m|nE^b\rangle = \varepsilon^\star|nE^b\rangle$. For our simplified *model* of the CD_3 group (remember, we assume it is rigid and it has exact C_3-symmetry) the effect of an even or *cyclic* permutation of the deuterons is exactly that of a rotation through $2\pi/3$, i.e., $\mathcal{P}_m\varphi = \varphi + 2\pi/3$. Note that a transposition of two deuterons has no meaning within this model.

When the potential height V_3 becomes finite, the eigenstates of $\mathcal{H}_R$ can no longer be chosen to be localized but, as $\mathcal{H}_R$ and $\mathcal{P}_m$ always commute, they can still be classified as $|nA\rangle, |nE^a\rangle, |nE^b\rangle$. The energies $E_{E^a}^{(n)}$ and $E_{E^b}^{(n)}$ are still degenerate but will differ from $E_A^{(n)}$. We define the *tunneling splitting* of the librational level n by

$$\Delta_n := E_{E^{a,b}}^{(n)} - E_A^{(n)}. \tag{8}$$

Specifically for the ground state $|0\rangle$ also the notation $\nu_t = \Delta_0/h$ is used. ν_t is called *tunnel frequency*. This frequency decreases roughly exponentially on increasing the potential height V_3. If V_3 is reasonably large in comparison to B, the low lying librational states can be approximated by harmonic oscillator functions. This means we can think of the ground states $|0A\rangle$, $|0E^a\rangle$, and $|0E^b\rangle$ as linear combinations of gaussians $\exp(-\varphi^2/\varphi_w^2)$, $\exp(-(\varphi - 2\pi/3)^2/\varphi_w^2)$, and $\exp(-(\varphi + 2\pi/3)^2/\varphi_w^2)$. They all have the same width φ_w, which depends on V_3. An instructive quantitative example of $|0A\rangle$ for $V_3 = 40$ meV is shown in Fig. 4 of Heuer [10].

We are now in a position to define the "tunneling regime" which appears in the title of this paper. It encompasses the regime of temperatures T where T is *low* enough so that in thermal equilibrium virtually all methyl groups of the macroscopic sample are in the librational ground state $|0\rangle$. On the other hand T should be high enough to satisfy the condition $k_B T \gg \Delta_0$ (k_B is the Boltzmann constant). This guarantees that

the high (!) temperature approximation is valid for the (thermal equilibrium) populations of the three states of the librational ground level $|0\rangle$. The orders of magnitude of $E^{(1)}_{A,E^a,E^b}$ and Δ_0 which we will encounter are $E^{(1)}_{A,E^a,E^B} \approx 10\,meV$ and $\Delta_0 \approx 10\,neV$. Both conditions will therefore be satisfied safely for 100 μK $\lesssim T \lesssim$ 30 K. *This temperature range we call the tunneling regime.* With regard to the space part of the basis functions of $\mathcal{H}$ it should be clear by now that in the tunneling regime we may restrict ourselves to the three lowest states of $\mathcal{H}_R$, i.e., to $|0A\rangle, |0E^a\rangle$ and $|0E^b\rangle$.

For $T = 0$ and thermal equilibrium only the lowest level $|0A\rangle$ will be occupied. We do not consider this situation. At the upper end of the tunneling regime phonon induced transitions to higher librational levels will set in appreciably, and this leads to observable damping phenomena, see Section 4.

2.3 The spin functions and the space-and-spin basis functions for diagonalizing $\mathcal{H}$

A natural start for selecting an appropriate set of spin functions are the eigenfunctions $|m_1m_2m_3\rangle := |m_1\rangle|m_2\rangle|m_3\rangle$ of $I_z^{(1)}, I_z^{(2)}$, and $I_z^{(3)}$, the eigenvalue of I_z^i being m_i. As $m_i = 0, \pm 1$, there are 27 of the functions $|m_1m_2m_3\rangle$.

For keeping the diagonalization of the $\mathcal{H}$-matrix as simple as possible it is helpful to arrange these functions in suitably *symmetry adapted* linear combinations. To see which combinations are suitable we consider the following operators (upper rows) and eigenvalues (lower rows):

I_z	=	$I_z^{(1)} + I_z^{(2)} + I_z^{(3)}$
M	=	$m_1 + m_2 + m_3$
$\boldsymbol{I}^2$	=	$(\boldsymbol{I}^{(1)} + \boldsymbol{I}^{(2)} + \boldsymbol{I}^{(3)})^2$
$I(I+1),\ I$	=	$3, 2, 1, 0$
$\mathcal{Z}$	=	$(I_z^{(1)})^2 + (I_z^{(2)})^2 + (I_z^{(3)})^2$
K	=	$m_1^2 + m_2^2 + m_3^2$
$\mathcal{P}_s$	=	permutation operator of spins
p	=	$1, \varepsilon, \varepsilon^\star$

The sets of operators $\mathcal{P}_s, I_z$ and $\boldsymbol{I}^2$ on the one, and $\mathcal{P}_s, I_z$ and $\mathcal{Z}$ on the other hand commute mutually, but $\mathcal{Z}$ and $\boldsymbol{I}^2$ do not commute. We may thus form linear combinations of the $|m_1m_2m_3\rangle$ which are simultaneously eigenfunctions of $\mathcal{P}_s$, I_z and $\boldsymbol{I}^2$ *or* of $\mathcal{P}_s, I_z$, and $\mathcal{Z}$. Diezemann [9], who treated spin relaxation in CD_3 groups, preferred the first set. Using this set the largest block in the $\mathcal{H}$-matrix is a 7 x 7 block. Using the second set the size of the largest block is only 3 x 3. Therefore we are going to use the second one.

From any triple of functions[1] $|m_1 = h, m_2 = k, m_3 = l\rangle$, $|m_1 = k, m_2 = l, m_3 = h\rangle$ and $|m_1 = l, m_2 = h, m_3 = k\rangle$ except those three with $h = k = l$ we can construct three orthogonal and normalized linear combinations which are simultaneously eigenfunctions of $I_z, \mathcal{Z}$ and $\mathcal{P}_s$. The recipe is in an obvious short hand notation

$$\begin{aligned} |hkl; A\rangle &:= \tfrac{1}{\sqrt{3}}(|hkl\rangle + |klh\rangle + |lhk\rangle), \\ |hkl; E^a\rangle &:= \tfrac{1}{\sqrt{3}}(|hkl\rangle + \varepsilon|klh\rangle + \varepsilon^*|lhk\rangle), \\ |hkl; E^b\rangle &:= \tfrac{1}{\sqrt{3}}(|hkl\rangle + \varepsilon^*|klh\rangle + \varepsilon|lhk\rangle). \end{aligned} \tag{9}$$

There are 24 such functions. The remaining three are $|hhh; A\rangle$. They all can be labeled with the triple of quantum numbers M, K and p. The function $|1, 1, -1; E^a\rangle$, for instance, has quantum numbers $M = 1, K = 3, p = \varepsilon$. The labeling of the functions $|hkl; \Gamma\rangle$, with $\Gamma = A, E^a$ and E^b, by M, K and p is *unique* except for $|1, 0, -1; \Gamma\rangle$ and $|-1, 0, 1; \Gamma\rangle$ which have the same quantum numbers $M = 0$ and $K = 2$. This indicates that there must be an additional quantum number, and an additional symmetry, which we have not taken into account so far. Indeed, the true Hamiltonian of the methyl group must be invariant under the *full* permutation group S_3, and the extra quantum number is related to odd transpositions of deuterons. We point out, however, that the functions in (9) are *not* eigenfunctions of the operators of odd transpositions of deuteron spins and that the extra quantum number is, therefore, not simply the eigenvalue of any such operator. Just for bookkeeping purposes we assign the extra label $p' = -1$ to the spin functions $|-1, 0, 1; \Gamma\rangle$ and $p' = +1$ to $|1, 0, -1; \Gamma\rangle$ and also $p' = +1$ to all other spin functions $|hkl; \Gamma\rangle$.

We must now combine the space functions $|0A\rangle$, $|0E^a\rangle$ and $|0E^b\rangle$ which are eigenfunctions of $\mathcal{P}_m$ with eigenvalues 1, ϵ and $\epsilon^\star$, respectively, with the spin functions $|hkl; A\rangle, |hkl; E^a\rangle$ and $|hkl; E^b\rangle$ which are eigenfunctions of $\mathcal{P}_s$ with eigenvalues 1, ϵ and $\epsilon^\star$. The

[1] m_1 is the eigenvalue of I_z^1, it *may* assume the values 0, +1, -1; h *is* a number.

Pauli principle allows only certain combinations. Basically it applies to odd transpositions, but it also applies to cyclic permutations $\mathcal{P} = \mathcal{P}_m \mathcal{P}_s$. Any stationary state function of, e.g., a three-identical-particle-system must be an eigenfunction of $\mathcal{P}$ with eigenvalue +1, regardless of whether the particles are bosons or fermions.

This means that only the following combinations of space and spin functions are possible

$$\begin{array}{ll} |0A\rangle & |hkl;A\rangle, \\ |0E^a\rangle & |hkl;E^b\rangle, \\ |0E^b\rangle & |hkl;E^a\rangle. \end{array}$$

There are 27 such combinations including, of course, those with $h = k = l$. They form the basis which we are going to use for diagonalizing the Hamiltonian matrix $\mathcal{H}$.

2.4 Hamiltonian matrix $\mathcal{H}$

It is obvious that $\mathcal{H}_R$ and $\mathcal{H}_Z$ are diagonal in "our" basis and it is trivial to calculate the respective matrix elements. Those of $\mathcal{H}_Z$ are $Mh\nu_L$. For fixing the origin of the energy scale we require (in analogy to $\mathcal{H}_Z, \mathcal{H}_Q$ and $\mathcal{H}_D$) that $tr\mathcal{H}_R = 0$. This implies

$$\langle A0|\mathcal{H}_R|0A\rangle = -\tfrac{2}{3}\Delta_0$$

and

$$\langle E^{a,b}0|\mathcal{H}_R|0E^{a,b}\rangle = +\tfrac{1}{3}\Delta_0. \tag{10}$$

$\mathcal{H}'_Q$ is *not diagonal* since $[\mathcal{P}_s, \mathcal{H}'_Q] \neq 0$ for $\cos\vartheta_1 \neq \cos\vartheta_2 \neq \cos\vartheta_3$. On the other hand $\mathcal{H}'_Q$ commutes with I_z and $\mathcal{Z}$. Therefore it mixes only states with identical quantum numbers M, K and, as it turns out, also of p'. As we have pointed out above, only the states $|hkl;A\rangle, |hkl;E^a\rangle$ and $|hkl;E^b\rangle$ have common quantum numbers M, K and p'. Therefore only such three states are mixed by $\mathcal{H}'_Q$. This explains why for "our" basis the largest block that must be diagonalized in the Hamiltonian matrix $\mathcal{H}$ will be a 3 x 3 block. The three functions $|0A\rangle|hhh;A\rangle$ are eigenfunctions of $\mathcal{H}'_Q$ and contribute 1 x 1 blocks to the $\mathcal{H}$-matrix.

For calculating the matrix elements of $\mathcal{H}'_Q$ we insert the r.h.s. of (3) into (2) and express the spin functions $|hkl;\Gamma\rangle$ by the r.h.s. of (9). We consider specifically the more interesting case where the three numbers h, k and l are not all equal. A matrix element of $\mathcal{H}'_Q$ can then be split up into 27 terms, 18 of which are zero because the spin functions $|hkl\rangle, |klh\rangle$ and $|lhk\rangle$ are orthogonal. Each term can further be split up into a spin– and a space part. The space parts are eventually expressed in terms of matrix elements of $\cos^2\vartheta_i(\varphi)$, $i = 1, \ldots, 3$ between the functions $\Psi_1^{(0)}, \Psi_2^{(0)}$ and $\Psi_3^{(0)}$ appearing on the r.h.s. of (7). Note that these functions are linear combinations of $|0A\rangle, |0E^a\rangle$ and $|0E^b\rangle$ which we know from the numerical solution of the Mathieu equation. For instance $\Psi_1^{(0)} = \frac{1}{\sqrt{3}}(|0A\rangle + |0E^a\rangle + |0E^b\rangle)$.

We first consider the *diagonal* elements of $\mathcal{H}'_Q$. It turns out that all 27 are independent of M, p and p'. They are equal to $(K-2)\cdot\beta$, where

$$\begin{aligned} \beta &= \tfrac{3}{8}hC_Q\{\cos^2\vartheta_1(\varphi) + \cos^2\vartheta_2(\varphi) \\ &\qquad + \cos^2\vartheta_3(\varphi) - 1\} \\ &= \tfrac{3}{8}hC_Q(3\cos^2\theta_m - 1)(1 - \tfrac{3}{2}\sin^2\zeta). \end{aligned} \tag{11}$$

The important point is that, as a consequence of the *assumed* C_3 symmetry of the methyl group, the *sum* $\sum_{i=1}^{3}\cos^2\vartheta_i(\varphi)$ does not depend on φ, (cf. second line of (11)). These matrix elements are, hence, independent of whether or not the functions $\Psi_1^{(0)}(\varphi), \ldots, \Psi_3^{(0)}(\varphi)$ are sharply localized.

If ζ equals the tetrahedral angle $\zeta_{tet} = 109,47°$ (which it will do at least approximately), we get

$$1 - \tfrac{3}{2}\sin^2\zeta_{tet} = -\tfrac{1}{3}$$

and

$$\beta = \beta_{tet} = -\tfrac{1}{8}hC_Q(3\cos^2\theta_m - 1). \tag{12}$$

2β is also the splitting which characterizes the high temperature spectrum of the CD_3 group.

The off-diagonal elements of $\mathcal{H}'_Q$ are more interesting. They do depend on the degree of localization of the spatial functions $\Psi_1^{(0)}(\varphi)$ etc. and their presence and size profoundly affects the deuteron NMR spectrum. The calculation of their spin parts is straightforward. A typical spatial matrix element is $\langle A0|\cos^2\vartheta_1(\varphi)|0E^a\rangle$. Such matrix elements can be evaluated (at least) on three descending levels of sophistication. First, they can be calculated *exactly* since we *know* the functions $|0A\rangle$ and $|0E^a\rangle$. On the second level of accuracy we may approximate $\Psi_1^{(0)}(\varphi)$ etc. by harmonic oscillator functions with a width φ_w. We shall give an example further below. The crudest approximation, although perfectly sufficient for most

purposes, is to substitute $\Psi_1^{(0)}(\varphi)$ by $\delta(\varphi)$ etc., i.e., by *pocket* functions.

In what follows we shall assume that the functions $\Psi_i^{(0)}(\varphi), i = 1, \ldots, 3$ do not overlap, i.e., we neglect terms of the type $\langle\Psi_1^{(0)}|\cos^2\vartheta_i(\varphi)|\Psi_2^{(0)}\rangle$. They are not exactly zero but are much smaller than the matrix elements $\langle\Psi_1^{(0)}|\cos^2\vartheta_i(\varphi)|\Psi_1^{(0)}\rangle$ which we retain. The latter we are going to denote by $\langle\cos^2\vartheta_i\rangle$.

We repeat: Matrix elements of $\mathcal{H}'_Q$ are nonzero only within the triples of states $|0\Gamma\rangle|hkl;\Gamma^\star\rangle$, $\Gamma = A, E^a, E^b$; $\Gamma^\star = A, E^b, E^a$. In the $\mathcal{H}$-matrix they thus appear in 3 x 3 blocks. Evidently the blocks can be labeled by M, K and p'. By properly choosing the phases of the *spin* functions $|hkl;\Gamma^\star\rangle$ and ordering the *basis* functions in the sequence $\Gamma = A, E^a, E^b$, all blocks appear in the form of

$$(K-2)\beta\begin{pmatrix}1&0&0\\0&1&0\\0&0&1\end{pmatrix}+\lambda\begin{pmatrix}0&\alpha&\alpha^\star\\\alpha^\star&0&\alpha\\\alpha&\alpha^\star&0\end{pmatrix},$$

where

$$\begin{aligned}\lambda &= +1 \quad \text{for} \quad K = 1,\\ \lambda &= -1 \quad \text{for} \quad K = 2,\\ \lambda &= \;\;0 \quad \text{for} \quad K = 3\end{aligned}$$

and

$$\alpha = \tfrac{3}{8}hC_Q(\langle\cos^2\vartheta_1\rangle + \varepsilon\langle\cos^2\vartheta_2\rangle + \varepsilon^\star\langle\cos^2\vartheta_3\rangle). \tag{13}$$

For deriving (13) we made use of the relations $\cos\vartheta_1(\varphi) = \cos\vartheta_2(\varphi - \frac{2\pi}{3}) = \cos\vartheta_3(\varphi + \frac{2\pi}{3})$ (and cyclic permutations of the indices 1, 2 and 3) which follow from (3).

The "proper" phases of the spin functions $|hkl;\Gamma^\star\rangle$ are obtained automatically if we choose the hkl for a given triple of M, K and p' in the following way (be aware that there *is* a choice!):

h	k	l	MKp'	h	k	l	MK	p'
1	1	1	3 3 1	−1	−1	−1	−3 3	1
0	1	1	2 2 1	0	−1	−1	−2 2	1
1	0	0	1 1 1	−1	0	0	−1 1	1
1	1	−1	1 3 1	−1	−1	1	−1 3	1
0	−1	1	0 2 1	0	1	−1	0 2	−1
0	0	0	0 0 1					

The 3 x 3 blocks of $\mathcal{H}_R + \mathcal{H}_Z + \mathcal{H}'_Q$ will thus be

$$(Mh\nu_L + (K-2)\beta)\begin{pmatrix}1&0&0\\0&1&0\\0&0&1\end{pmatrix} + \frac{h\nu_t}{3}\begin{pmatrix}-2&0&0\\0&1&0\\0&0&1\end{pmatrix} + \lambda\begin{pmatrix}0&\alpha&\alpha^\star\\\alpha^\star&0&\alpha\\\alpha&\alpha^\star&0\end{pmatrix}.$$

We recognize that the tunnel frequency ν_t and the (complex) quantity α will be decisive for the shape of the NMR spectrum of a CD_3 group in the tunneling regime. There are two simple cases. The first is obtained when $h\nu_t$ is much smaller than $|\alpha|$. All three states $|0\Gamma\rangle|hkl;\Gamma^\star\rangle, \Gamma = A, E^a, E^b$ will then be strongly mixed. In the limiting case $\nu_t = 0$ the spectrum will be that of three independent deuterons whose C–D bonds have fixed orientations in space. The secular equation we must solve to cover this case is obviously

$$E^3 - 3E\alpha\alpha^\star - (\alpha^\star)^3 - \alpha^3 = 0. \tag{14}$$

The solutions are

$$E_1 = \alpha + \alpha^\star = \tfrac{3}{8}hC_Q\left(2\langle\cos^2\vartheta_1\rangle - \langle\cos^2\vartheta_2\rangle - \langle\cos^2\vartheta_3\rangle\right), \tag{15}$$

and E_2, E_3 are obtained by cyclically permuting the indices. By including E_1, E_2, E_3 into the energy level diagram, and not forgetting λ, one indeed gets the spectrum of three independent, immobile deuterons.

The other limiting case is that where $h\nu_t \gg |\alpha|$. We may now neglect the off-diagonal elements connecting $|0A\rangle|hkl;A\rangle$ with $|0E^a\rangle|hkl;E^b\rangle$ and $|0E^b\rangle|hkl;E^a\rangle$, but we must not neglect the element connecting the latter two states because the respective diagonal elements in the matrix are identical. This means that the level diagram can be thought of consisting of two independent parts, an "A"-part with 11 states (two are degenerate) and an "E"-part with 16 states. The two parts are shifted with respect to each other by $h\nu_t$. The operator which drives transitions in an NMR experiment is $I_x = I_x^{(1)} + I_x^{(2)} + I_x^{(3)}$. It is totally symmetric under $\mathcal{P}_s$. Therefore it induces transitions only between the A-states on the one, and between the E-states on the other hand, and the spectrum itself consists of independent A- and E-parts.

$\mathcal{H}_Z$ and the diagonal part of $\mathcal{H}'_Q$ leave all the E-levels twofold degenerate. The off-diagonal part of

$\mathcal{H}'_Q$ lifts this degeneracy except for the E-states with $K = 3$. The respective level shifts are given by the solutions of the secular equation

$$E^2 - \alpha\alpha^\star = 0 \tag{16}$$

with the obvious solutions

$$\begin{aligned} E_{1,2} &= \pm|\alpha| \\ &= \pm\frac{3}{8}hC_Q\{\langle\cos^2\vartheta_1\rangle^2 + \langle\cos^2\vartheta_2\rangle^2 \\ &\quad + \langle\cos^2\vartheta_3\rangle^2 - \langle\cos^2\vartheta_1\rangle\langle\cos^2\vartheta_2\rangle \\ &\quad - \langle\cos^2\vartheta_1\rangle\langle\cos^2\vartheta_3\rangle \\ &\quad - \langle\cos^2\vartheta_2\rangle\langle\cos^2\vartheta_3\rangle\}. \end{aligned} \tag{17}$$

The corresponding spectrum is that shown in Figure 1. The pocket function approximation of $\Psi_1^{(0)}(\varphi)$ implies $\langle\cos^2\vartheta_i\rangle = \cos^2\vartheta_i(0)$. After a tedious calculation we get in this approximation

$$\begin{aligned} |\alpha| = \tfrac{9}{8}hC_Q \sin\zeta \sin\theta_m \big(&\cos^2\zeta\cos^2\theta_m \\ &+ \tfrac{1}{16}\sin^2\zeta\sin^2\theta_m \\ &+ \tfrac{1}{8}\sin 2\zeta\sin 2\theta_m\cos 3\phi_m\big)^{1/2}, \end{aligned} \tag{18}$$

which becomes for $\zeta = \zeta_{tet}$

$$\begin{aligned} |\alpha_{tet}| = \tfrac{1}{4}hC_Q \sin\theta_m \\ \cdot\sqrt{1 + \cos^2\theta_m - \sqrt{2}\sin 2\theta_m\cos 3\phi_m}. \end{aligned} \tag{19}$$

The remarkable and, at the same time, *natural* thing about (19) is that $|\alpha|$ depends on ϕ_m in the form of $\cos 3\phi_m$. It means that it is irrelevant which of the three C–D bonds we select for defining the direction of the x_m axis of the molecular axis system. Remember that we have defined this direction with respect to a minimum of the potential $V(\varphi)$. In the δ-function approximation of $\Psi_1^{(0)}(\varphi)$ this is equivalent to saying that the x_m-axis is parallel to the projection of *a* C–D bond on the x_m, y_m-plane for the *equilibrium orientation* of the CD_3 group. Note that, even if we know the X-ray structure of a crystal, we usually do not know the equilibrium orientation of the methyl group; therefore we actually do not know ϕ_m and the direction of x_m. Below we show that the dependence of $|\alpha|$ on the orientation of the applied field in a *crystal fixed* axes system allows us to deduce the equilibrium orientation of the methyl group.

Before discussing the intermediate case, i.e., when $h\nu_t$ is neither very much larger nor very much smaller than $|\alpha|$, we briefly consider what happens if we give up the δ-function approximation of $\Psi_1^{(0)}$ and use, instead, the harmonic oscillator function approximation. The matrix elements in question are

$$\begin{aligned} \langle\Psi_1^{(0)}|\cos^2\vartheta_i(\varphi)|\Psi_1^{(0)}\rangle = N\int_{-\pi}^{+\pi}&\exp(-2\varphi^2/\varphi_w^2) \\ &\cdot\cos^2\vartheta_i(\varphi)\mathrm{d}\varphi, \end{aligned}$$

where N is a normalization constant and $i = 1, 2, 3$.

If this approximation is to make sense at all, the gaussian is sufficiently sharp so that we can shift, on the one hand, the limits of integration to $\pm\infty$ and, on the other hand, we can expand the $\cos^n\varphi$ and $\sin^n\varphi$ terms in $\cos^2\vartheta_i(\varphi)$ and drop terms higher than φ^2. The result for $i = 1$ is then

$$\begin{aligned} \langle\Psi_1^{(0)}|\cos^2\vartheta_1(\varphi)|\Psi_1^{(0)}\rangle = \cos^2\vartheta_1(0) - \tfrac{1}{4}\varphi_w^2 \\ \cdot\big(\sin^2\zeta\sin^2\theta_m\cos 2\phi_m \\ + \tfrac{1}{4}\sin 2\zeta\sin 2\theta_m\cos\phi_m\big). \end{aligned} \tag{20}$$

The correction represented by the second term in (20) can easily be taken into account in numerical calculations of deuteron NMR spectra. Note that the matrix element in (20) is not measured independently of others; therefore ϕ_m need not appear in the form of $\cos 3\phi_m$ or $\sin 3\phi_m$.

2.5 The intermediate case: $h\nu_t$ comparable to $|\alpha|$

When the tunnel frequency ν_t, multiplied by h, is neither very much larger nor very much smaller than $|\alpha|$ we must face the general secular equation of a 3×3 block of the $\mathscr{H}$-matrix. It reads

$$\begin{aligned} 0 = E^3 - 3E(\alpha\alpha^\star + \tfrac{1}{9}(h\nu_t)^2) \\ - [\lambda^3(\alpha^3 + (\alpha^\star)^3) - \tfrac{2}{27}(h\nu_t)^3] \end{aligned} \tag{21}$$

or, with obvious abbreviations a and b,

$$E^3 - 3Ea - b = 0. \tag{22}$$

It is easy to show that $b^2 - 4a^3$ is always negative. Then the solutions of (22) are $E_1 = A + A^*$, $E_2 = \varepsilon A + \varepsilon^* A^*$, $E_3 = \varepsilon^* A + \varepsilon A^*$, where $A = [\frac{1}{2}(b + i\sqrt{4a^3 - b^2})]^{1/3}$. The inherent symmetry of

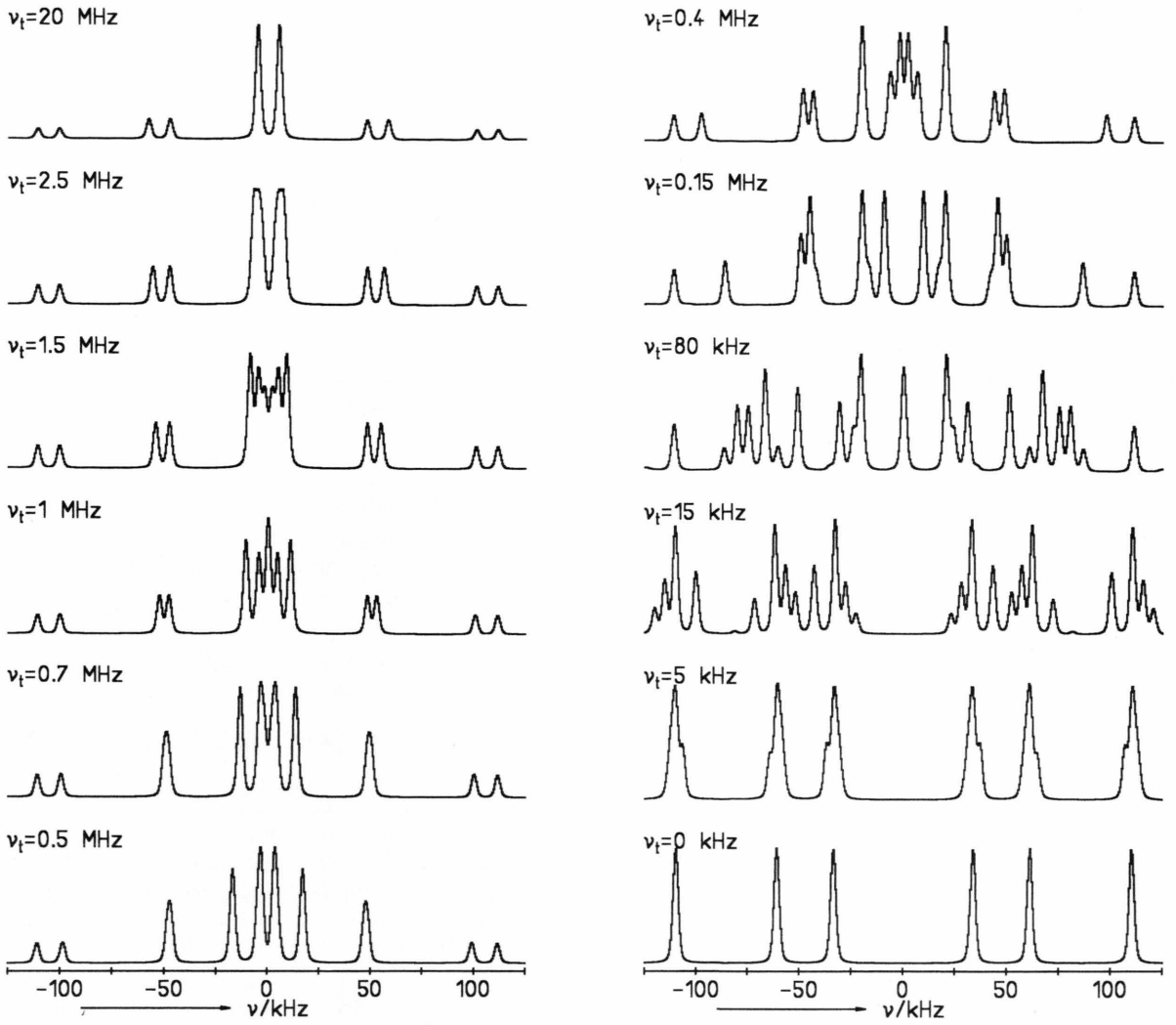

Fig. 3. The variation of the shape of the deuteron NMR spectra as a function of ν_t in the tunneling regime. For this series of simulations we chose the polar angles $\theta_m = 60°$ and $\phi_m = 47°$ for the orientation of $\boldsymbol{B}_0$, C_Q=160 kHz, an intra-group dipole-dipole coupling strength of 0.79 kHz, and an artificial but realistic line broadening of 3 kHz.

the problem is better seen if we write $A = |A| \exp(i\Phi)$. $|A| = \sqrt{a}$, $\cos 3\Phi = -b/(2a^{\frac{3}{2}})$. Then

$$E_1 = 2\sqrt{a}\cos\Phi,$$
$$E_2 = 2\sqrt{a}\cos(\Phi + 2\pi/3),$$
$$E_3 = 2\sqrt{a}\cos(\Phi - 2\pi/3).$$

The splitting $E_2 - E_3$ is $-2\sqrt{3a}\sin\Phi$. In the limit $\nu_t \to \infty$ we have $\sqrt{a} \to \frac{1}{3}h\nu_t$, $\sin\Phi \to -\sqrt{3}|\alpha|/(h\nu_t)$. This leads to $E_2 - E_3 = 2|\alpha|$ which agrees with (17). Thus the spectra can, in principle, be calculated analytically for any ν_t. However, it is still more convenient to use numerical methods.

We have written a program that solves the secular equation including the intramolecular dipole-dipole terms and simulates the deuteron NMR spectrum for arbitrary values of ν_t, θ_m and ϕ_m (i.e., α and β). The spectral intensity at a transition frequency $\nu_{i,f} = (E_i - E_f)/h$ is proportional to $|\langle f|I_x|i\rangle|^2$, where $|i\rangle$ and $|f\rangle$ are eigenfunctions of $\mathcal{H}$ with eigenvalues E_i and E_f, respectively. Lorentzian or gaussian line broadening is introduced artificially. Figure 3 shows, for a more or less arbitrary, fixed orientation of $\boldsymbol{B}_0$ ($\theta_m = 60°; \phi_m = 47°$) how the deuteron NMR spectrum changes when the tunnel frequency is lowered from 20 MHz down to zero. For this orientation

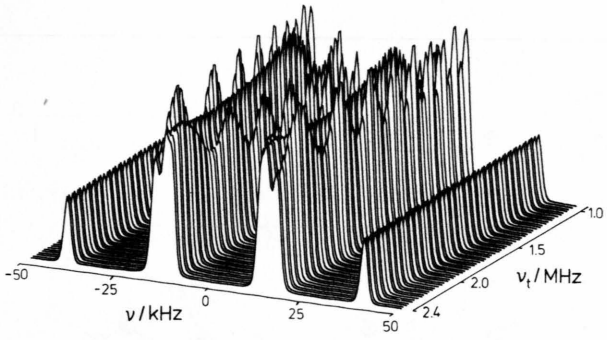

Fig. 4. Variation of the inner part of the deuteron NMR spectrum of the CD_3 group as a function of ν_t. The orientation of $\boldsymbol{B}_0$ is $\theta_m = 70°$, $\phi_m = 60°$. Note the oscillatory behaviour of the intensities of the components of inner lines.

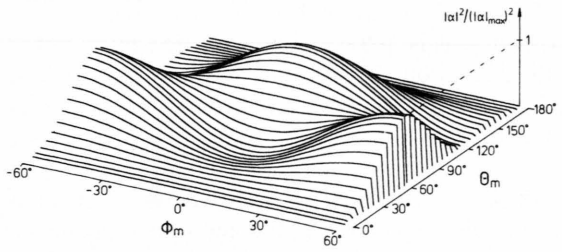

Fig. 5. Dependence of $|\alpha|^2$, normalized to $|\alpha|^2_{max}$, on the polar angles θ_m and ϕ_m of $\boldsymbol{B}_0$ in the molecular axes system.

of $\boldsymbol{B}_0$ the key quantity $|\alpha|/h$ equals 39.9 kHz. We have set the linewidth arbitrarily, but realistically, to 3 kHz. The spectra are scaled such that the *largest* lines have the same height in all spectra.

For $\nu_t = 20$ MHz we get a spectrum of the type of Figure 1. It is characteristic of the case $h\nu_t \gg |\alpha|$. It does not allow to tell *how* large ν_t is, it only gives a lower limit. On lowering ν_t we see the first pronounced change in the spectrum when ν_t reaches about 2.5 MHz: the large central $\pm\beta$ lines split in *two*, and starting at about $\nu_t = 1.5$ MHz, even in *three* components. In this range of ν_t the splittings of the $\pm\beta$ lines are proportional to $|\alpha|^2/h\nu_t$. If we observe such splittings in experimental spectra we may infer the tunnel frequency. The relative size of the line components varies in an oscillatory manner as a function of ν_t. This is shown in Figure 4. This behaviour can be exploited for improving the accuracy of the determination of the tunnel frequency. We now return to the discussion of Figure 3.

When ν_t becomes about 1 MHz, marked changes become also visible in the $\pm|\alpha|$ pairs of lines: the pair splitting obviously deviates from 2β. For $\nu_t \lesssim 500$ kHz the distinction between the A and the E-part of the spectrum definitively gets lost and we observe a whole "forest" of lines. Only when the tunnel frequency drops below 15 kHz the spectrum starts to resemble that of an immobile CD_3 group, i.e., the spectrum for $\nu_t = 0$. As long as ν_t is larger than the linewidth we see significant features in the spectrum, which can be taken as fingerprints of tunneling.

The important point is that in the whole range 2 MHz $\gtrsim \nu_t \gtrsim$ 5 kHz the shape of the spectrum depends in a sensitive way on ν_t. This means that the tunnel frequency can be deduced from an experimental spectrum provided that ν_t falls in that range. It is worth emphasising that the shape of the spectrum also depends on the orientation of $\boldsymbol{B}_0$. The key parameter α actually varies strongly with the orientation of $\boldsymbol{B}_0$. This is shown in Fig. 5, where $|\alpha|^2/(|\alpha|_{\max})^2$ is plotted versus θ_m and ϕ_m (we assumed $\zeta = \zeta_{tet}$).

As is intuitively clear, we find that $|\alpha| = 0$ for $\theta_m = 0°$ and 180°. A maximum occurs for $\phi_m = 0$ (which implies $\cos^2 \vartheta_2(0) = \cos^2 \vartheta_3(0)$) and $\theta_m = 117.37°$. By symmetry other, equally large maxima are found at $\phi_m = \pm 60°$ and $\theta_m = 180° - 117.37° = 62.63°$. If one is interested, as we are, in measuring (comparatively) large tunnel frequencies it is evidently favourable to orient the crystal such that $|\alpha|$ is near one of its maxima.

3. Experimental

3.1 NMR

All the measurements to be reported in this paper were carried out with a homebuilt FT-spectrometer whose central piece is an 11 Tesla magnet from BRUKER, Karlsruhe. The deuteron Larmor frequency is thus 72.1 MHz. With a cryostat (inner diameter 30 mm, outer diameter 50 mm) and an ITC-4 temperature controller, both from OXFORD INSTRUMENTS, we cover the temperature range from 300 K down to about 5 K. The stability of T is better than 0.1 K. We measure T with a calibrated semiconductor sensor from LAKESHORE placed at a (horizontal) distance of 12 mm from the sample.

We record spectra by tracking and Fourier transforming free induction decays excited by rf-pulses with a duration of 1.5 μs. These are 60° pulses; $\pi/2$ pulses would only barely cover the frequency range of interest. We avoid working with quadrupolar echoes because in the tunneling regime the echo spectra show a complicated phase behaviour: depending on the pulse separation in the echo pulse sequence, the $|\alpha|$-lines may appear in emission (!) and the $2|\alpha|$-lines in dispersion [5], [6]. We shall report about these effects, which we understand, under separate cover.

The NMR probe head is equipped with a goniometer which allows to rotate the sample about an axis perpendicular to the applied field. The accuracy of the angle setting is about 0.2°. The goniometer works in the whole temperature range of the cryostat. The sample is fixed in a standard 5 mm NMR tube.

3.2 Samples

For this study we looked for a compound which contains methyl groups, is simple, and promised that the tunnel frequency is large enough for seeing evidence of CD_3 tunneling. The criteria for *simplicity* were (i) feasibility of synthesizing the compound with 99% deuterated methyl groups; (ii) ease of growing crystals large enough to make them suitable for single crystal deuteron NMR (i.e., smallest dimension of crystal $\gtrsim$ 1 mm) and (iii) small number N of magnetically inequivalent methyl groups. The systems in which we saw CD_3 tunneling previously are not simple in this sense: CD_3-methanol guests in hydrochinon [5] and (CD_3)-paraxylene guests in Dianin's inclusion compound [6] possess, respectively, three and six available sites in their host crystals. These sites are, moreover, rather ill-defined [13]. We also felt that the classical systems where, in powder samples, methyl tunneling has been observed previously, namely copper acetate monohydrate [14] and toluene [15], [16], are anything but simple.

Therefore we selected aspirin (acetylsalicylic acid). The methyl group in aspirin has the same local environment as it has in the acetates. This made us hope that the tunnel frequency would be "reasonably" high. Aspirin is also "simple": aspirin CD_3 *can* be synthesized and crystals *can* be grown. The structure is monoclinic with two crystallographically equivalent molecules in the unit cell. N is thus two, but if the applied magnetic field lies *in* the monoclinic plane of the crystal, we are looking with NMR at effectively a single molecule, or a single CD_3 group.

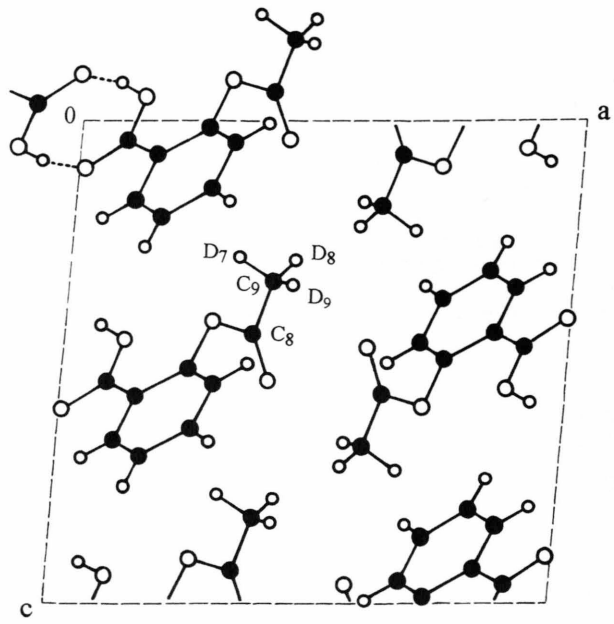

Fig. 6. Projection of the unit cell of acetylsalicylic acid (aspirin) on the ac-plane. The space group is P $2_1/c$; a = 11.446Å, b = 6.596Å, c = 11.388Å, and β = 95.55°. The labeling of the atoms follows that of Wheatley [17]. All molecular directions specified in this paper refer to *that* molecule in the unit cell whose atoms are labeled in this figure.

A projection on the ac-plane of the unit cell of aspirin, following the X-ray structure of Wheatley [17], is shown in Figure 6. This figure also provides an idea of the *molecular* structure of aspirin. The labeling of the atoms of interest follows the scheme of Wheatley. We shall often need to specify directions in crystals of aspirin. To do this we introduce the so-called standard orthogonal (SO-) system with $x_{SO} \parallel a$, $y_{SO} \parallel b$ and $z_{SO} \parallel c^\star$.

We synthesized aspirin-CD_3 and grew crystals from a solution in ether. The synthesis will be described separately together with that of aspirin-CH_2D, which we currently investigate. Actually it turned out that the quality of only one crystal specimen of the crop was good enough for the present work. Its size was approximately 4x5x12 mm^3. We oriented it using an optical goniometer. The b-axis, which is the *monoclinic* axis, could be identified unambiguously. On the other hand we could not distinguish the a- and

c-axes because the lengths of these axes are almost equal, $a = 11.446$ Å and $c = 11.388$ Å [17]. We cut this crystal in two pieces and fixed one in a sample tube such that it could be rotated about the *b*-axis. In what follows it will be called the B-crystal. The other piece was prepared such that it could be rotated about the (110)-axis. It will be called the AB-crystal. At this stage we were not sure, however, whether the rotation axis of this crystal is the (110) or the (011) axis. We resolved this ambiguity by deuteron NMR. This will be explained at the beginning of the next section.

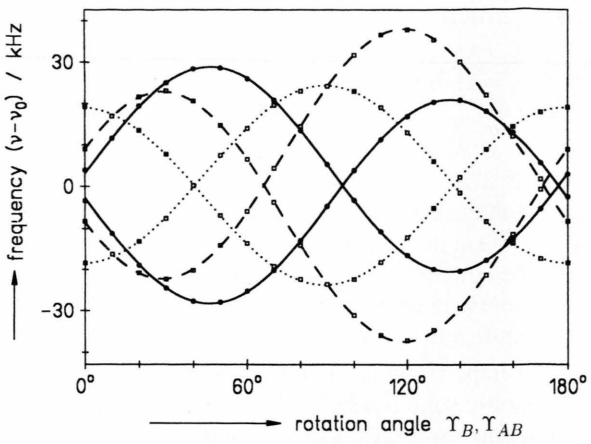

Fig. 7. Rotation pattern of the spectral line positions of the B- and AB-crystals at $T = 50$ K. The experimental points are given, respectively, by stars and squares. The common fit to a traceless 2nd rank EFG tensor is represented by the full (B-crystal) and the dashed and dotted curves (AB-crystal). For the B-crystal the magnetic field $\boldsymbol{B}_0$ moves about the $-b$-axis and is parallel to the $-c$-axis at $\Upsilon_B = 29.7°$. For the AB-crystal the rotation axis has polar coordinates $\theta_\Upsilon = 92.2°, \phi_\Upsilon = 238.4°$ in the SO-frame and the path of $\boldsymbol{B}_0$ crosses the monoclinic plane (near the *c*-axis) at $\Upsilon_{AB} = 90°$.

4. Results and Discussion

4.1 Spectra of aspirin-CD_3 at $T \geq 50$ K; motionally averaged EFG tensor; orientation of the (pseudo-) C_3-axis of the CD_3 group

For finding out whether the rotation axis of the AB crystal is (110) or (011) we recorded spectra from both crystals at room temperature, incrementing the rotation angle in steps of 10°. The spectra from the B crystal consisted always of a single pair of lines. This proves that the rotation axis coincides indeed with the monoclinic *b*-axis within a small fraction of a degree. As expected, the spectra from the AB crystal consisted in general of *two* pairs of lines.

The rotation patterns of the pair splittings from both crystals can be used to calculate a general symmetric second rank interaction tensor. If we assume that the rotation axis of the AB crystal is (011), the *trace* of this tensor turns out to be of similar size as the magnitudes of the diagonal elements. This is incompatible with an EFG tensor as the interaction tensor. If, on the other hand, we assume that the rotation axis is the (110) direction, the trace of the interaction tensor turns out to be zero within experimental errors. Thus, the rotation axis *is* (110), or at least nearly so. For finding its direction more precisely, we searched in the *neighbourhood* of (110) the direction which minimized the standard deviation between the measured and calculated splittings using, of course, a *traceless* EFG tensor for calculating the splittings. In the SO-frame this direction, which must be that of the "true" rotation axis, turned out to have polar angles $\theta_{AB} = 91.5°$ and $\phi_{AB} = 239.1°$ while, following [17], the polar angles of (110) are $\theta_{110} = 87.22°$ and $\phi_{110} = 240.05°$.

The fitted EFG tensor contained a surprise: it deviates significantly from axial symmetry, the asymmetry factor η being 0.119 ± 0.005. Remember that the *model* of the CD_3 group introduced in Sect. 2 implies $\eta = 0$. The C_3-axis is thus only a pseudo-threefold axis. A hypothesis explaining the result $\eta \neq 0$ is that the C_3-axis carries out oscillations about the C_8–O axis (cf. Figure 6) . To account for the size of η the amplitude of these oscillations would have to be somewhere between 15° and 20° [18]. For testing out this hypothesis we repeated the measurements at $T = 50$ K. The idea was to freeze out the hypothetical oscillations. Because of onset of tunneling, we did not go to a still lower temperature. In Fig. 7 we show the results. The line positions in the spectra of the B- and AB-crystals are plotted versus the rotation angle. These data give immediate evidence that the (motionally averaged) EFG tensor giving rise to the splittings is not axially symmetric: if it were, the full, the dotted and the dashed curves would have a maximum (not necessarily the *largest* one) *of the same size*. Evidently the three curves do not have maxima

of equal size. The quantitative analysis of the data in Fig. 7 yields a (motionally averaged) EFG tensor with $\eta = 0.098 \pm 0.005$ and a quadrupole coupling constant $\bar{C}_Q = (55.8 \pm 0.3)$ kHz.

The asymmetry is thus smaller at 50 K than at 300 K, but it is still substantial. Therefore we hesitate to maintain that the hypothesis formulated above is correct. Another possibility leading to $\eta \neq 0$ is that the assumed equilateral triangle formed by the deuterons is distorted in aspirin. A distortion of not more than 2° is sufficient to account for the observed value of η.

We hope to settle the question of the non-axially symmetric deuteron EFG tensor in aspirin with measurements on aspirin-CH_2D, where we suspect that tunneling is suppressed due to the loss of the S_3-permutation symmetry. If this turns out to be true, there is a chance to measure the EFG tensors of immobile deuterons in, hopefully, all three positions in the methyl group. Such measurements are under way. For the time being we just accept that the theory developed in Sect. 2 is based on assumptions which are not strictly valid for the methyl groups in aspirin. We postpone an attempt to extend the theory until the origin of the nonzero asymmetry factor has been clarified.

The other noteworthy feature of the motionally averaged EFG tensor is the direction θ_u, ϕ_u of the *unique* principal axis. This is the principal axis which *would be* the symmetry axis of the EFG tensor if it *were* exactly axially symmetric. We expect this direction to be parallel within a degree or so to the direction θ_b, ϕ_b of the bond between carbons C_8 and C_9, cf. Figure 6. The analysis of the data in Fig. 7 gives $\theta_u = 33.8°, \phi_u = 124.9°$ while, according to reference [17], $\theta_b = 33.0°, \phi_b = 126.5°$. The close agreement between the two sets of numbers is the final proof that we have correctly assigned and localized the rotation axes of our crystals. It also proves that the *modification* of our crystals is the same as that whose structure was solved by Wheatley. In view of the polymorphism of aspirin [19] this is a nontrivial statement.

4.2 The tunneling regime; spectra of the B-crystal at $T = 12.5$ K; equilibrium orientation of the CD_3 group

We have recorded spectra from the B-crystal at $T = 12.5$ K, incrementing the rotation angle Υ in steps of 10°. In the left column of Fig. 8 we show a selection

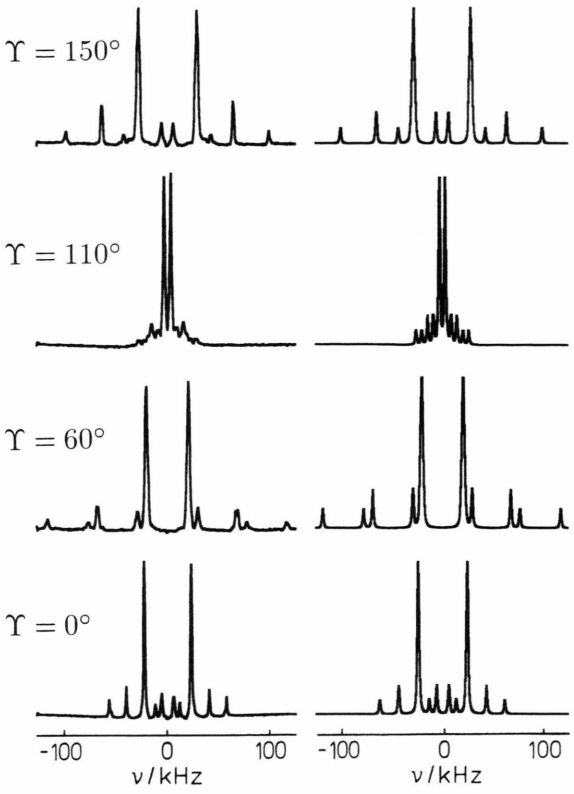

Fig. 8. Left column: selected deuteron NMR spectra of the B-crystal recorded at $T = 12.5$ K. The predicted strong $\pm\beta$, weak $\pm(|\alpha| \pm \beta)$ and weakest $\pm(2|\alpha| \pm \beta)$ lines are clearly identifiable. In the spectrum for $\Upsilon = 60°$ the lines appear in the same order as in the theoretical prototype tunneling spectrum shown in Figure 1. The rotation angles Υ refer to Figure 9. Right column: simulations of spectra, stipulating ν_t=2.7 MHz. The polar angles θ_m and ϕ_m were adjusted.

of these spectra. They provide unambiguous evidence that at $T = 12.5$ K the methyl groups in aspirin are in the tunneling regime and that the tunnel frequency is large in the sense of Section 2. This is the key point. The spectrum for $\Upsilon = 60°$, in particular, displays beautifully the characteristic features of the prototype tunneling spectrum in Figure 1.

The spectra in the right hand column of Fig. 8 are *simulations* which were computed with the same program as that used for producing Figure 3. The quadrupole coupling constant C_Q was set at 170 kHz and the tunnel frequency at $\nu_t = 2.7$ MHz, see below. The parameters available for variation to get a match with the corresponding experimental spectrum

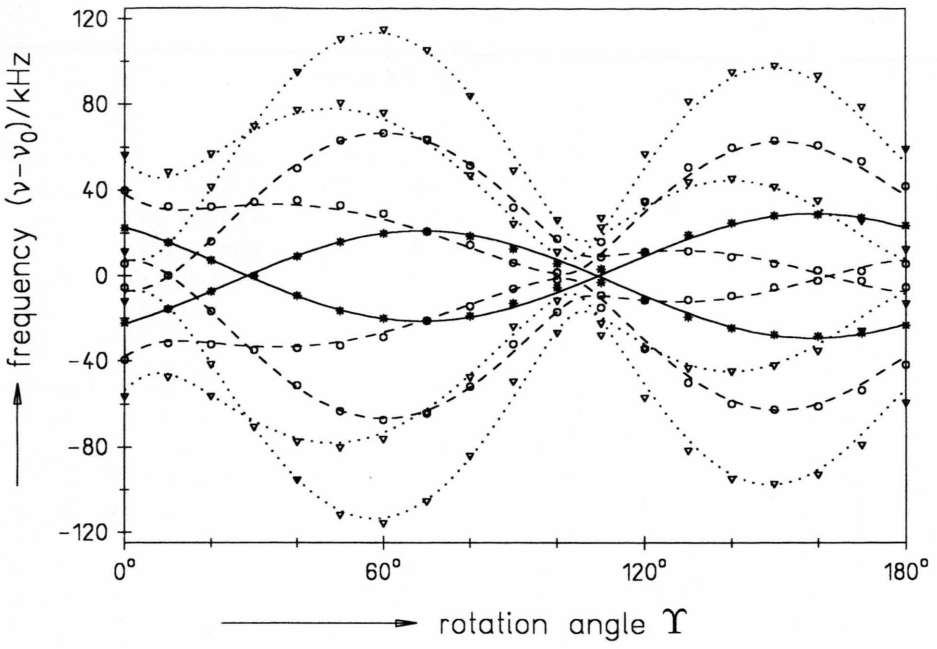

Fig. 9. Rotation pattern of the spectral line positions of the B-crystal at T = 12.5 K. The magnetic field moves about the b-axis and is parallel to the c^*-axis at $\Upsilon = 1.2°$. The $\pm\beta$, $\pm(|\alpha| \pm \beta)$ and $\pm(2|\alpha| \pm \beta)$ lines are represented, respectively, by stars, circles and triangles. The full, dashed and dotted curves are fits based on (12) and (19).

are α and β, or θ_m and ϕ_m. We think that the agreement between simulated and experimental spectra is quite impressive although some discrepancies in the intensities of, in particular, the E-lines cannot be overlooked.

In fact, the angles θ_m and ϕ_m are not free parameters. θ_m is fixed by the rotation axis (the b-axis) and the rotation angle Υ. On the other hand, ϕ_m is known only up to a constant since the X-ray structure of aspirin (and probably of most other compounds containing methyl groups) is not accurate enough for establishing definitively the equilibrium orientation of the methyl group. We shall now use the measured dependence of $|\alpha|$ on the rotation angle Υ for determining this equilibrium orientation.

In Fig. 9 we have plotted the positions of all lines in the spectra of the B-crystal versus the rotation angle Υ. We fitted the experimental data to the "high-tunnel-frequency" case, in which the line positions are given by $\pm\beta, \pm(|\alpha| \pm \beta)$ and $\pm(2|\alpha| \pm \beta)$. The fit is shown by the full, dashed and dotted curves. It was obtained in the following way: β depends (apart from C_Q) only on θ_m, which is a known function of Υ. This means that, apart from a scaling due to C_Q, there is no freedom at all to fit the $\pm\beta$ lines. In the expression for $|\alpha|$ (actually $|\alpha_{tet}|$, (19)), there appears the angle ϕ_m. For linking ϕ_m to Υ we introduce the orthogonal axes x_c and y_c in the x_m, y_m plane (the index c stands for *crystal* fixed). The axis x_c is defined as the line of intersection of the known x_m, y_m plane with the monoclinic plane of the crystal. For the sake of definiteness we also require that the polar angle of the positive x_c-axis in the SO-frame be zero. The polar angles of $\boldsymbol{B}_0$ in the righthanded, orthogonal frame $x_c, y_c, z_c = z_m$ are $\theta_c = \theta_m$ and ϕ_c. The latter depends, as θ_c does, in a known way on Υ, thus $\phi_c = \phi_c(\Upsilon)$. We may now express ϕ_m as

$$\phi_m(\Upsilon) = \phi_c(\Upsilon) - \phi_0, \tag{23}$$

where ϕ_0 is a constant. It is the angle between the (known) x_c- and the (so far unknown) x_m-axis. We may find ϕ_0, and thus x_m, and thus the equilibrium orientation of the methyl group, by fitting the data in

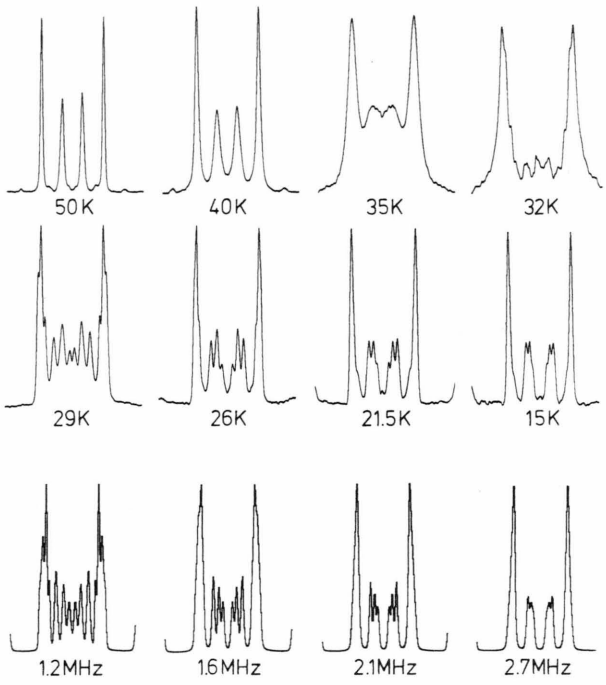

Fig. 10. Top and center row: temperature dependence of the inner ± 50 kHz range of the deuteron spectrum of the AB-crystal. The crystal orientation corresponds to $\Upsilon_{AB} = 30°$ in Figure 7. Bottom row: simulations of the center row of spectra. The tunnel frequency is the only fitting parameter, the optimum value is given below each spectrum. The experimental spectra indicate that not only the tunnel frequency changes with temperature, but also the width of the individual resonances.

Fig. 9 to $|\alpha(\Upsilon)|$ and treating ϕ_0 as the fitting parameter. This we have done. The curves in Fig. 9 have been obtained with $\phi_0 = 75°$. The sensitivity of the fit procedure is good enough to say that this number is valid to within $\pm 2°$.

Table 1. Polar angles θ_{SO} and ϕ_{SO} of the C–D bond directions for the equilibrium orientation of the CD_3 group in aspirin*.

	Deuteron NMR		X-ray diffraction	
	θ_{SO}	ϕ_{SO}	θ_{SO}	ϕ_{SO}
C_9 - D_7	120°	205°	126°	196°
C_9 - D_8	76°	310°	88°	295°
C_9 - D_9	125°	54°	128°	47°

*The numbers are for *that* of the two molecules in the unit cell whose atomic positions are *directly* given in [17].

The knowledge of ϕ_0 enables us now to specify the *equilibrium* C–D bond directions in aspirin. They are given in Table 1 together with the respective diffraction results [17].

We recognize a rough agreement between our deuteron NMR and the X-ray results. According to the latter the D–C_9–D and D–C_9–C_8 bond angles differ among themselves by more than 20°. This is unrealistic and we think, therefore, that our NMR results with their built-in tetrahedral symmetry are more trustworthy.

We close this section with a comment on the quality of the fit of the data in Fig. 9, for which we have used (12) and (19), respectively, for β and $|\alpha|$. A perfect fit is definitely not possible. It is hardly improved by using (18) for $|\alpha|$ and treating ζ as an adjustable parameter. The splitting of the $\pm|\alpha|$ and $\pm 2|\alpha|$ resonances, which theoretically equals 2β, is consistently smaller by about 1 kHz in the experimental spectra than the separation of the $\pm\beta$ pair of lines. Even the $\pm\beta$ lines deviate noticeably from the anticipated $\beta(\Upsilon) = C_1 + C_c \cos 2\Upsilon + C_s \sin 2\Upsilon$ behaviour with C_1, C_c, and C_s being constants. At 50 K the line splittings obeyed this basic relation well within experimental errors.

4.3 Temperature dependence of spectra; inference of the tunnel frequency

In this section we set out to infer the tunnel frequency ν_t and, eventually, its temperature dependence from the shape of the deuteron NMR spectra. In the previous subsection we concluded that ν_t must be large in the sense of Sect. 2, at least at $T = 12.5$ K. In Sect. 2 we learned that, if ν_t is "large", there are favourable and less favourable orientations of $\boldsymbol{B}_0$ for inferring ν_t. It turns out that all orientations of $\boldsymbol{B}_0$ which are accessible with the B-crystal are not particularly favourable. The situation is different for the AB-crystal in which NMR "sees" two methyl groups with two differently oriented molecular axes systems. If we choose the rotation angle $\Upsilon_{AB} = 30°$ (cf. Fig. 7) we get $\theta_m = 62°, \phi_m = 55°$ for one group while $\theta_m = 94.5°, \phi_m = 22.8°$ for the other (that with the larger splitting). A look at Fig. 5 reveals that for the former group $\boldsymbol{B}_0$ is almost in the optimum orientation, i.e., $|\alpha|$ is close to its maximum. As a matter of fact $|\alpha(\theta_m = 62°, \phi_m = 55°)|/C_Q = 1.3544$, while the maximum value is 1.3660.

For this orientation $\Upsilon_{AB} = 30°$ of the AB-crystal we have recorded spectra in the range 5 K $\lesssim T \lesssim$ 50 K at small increments of T. In the top two rows of Fig. 10 we show eight of them. Only the inner ±50 kHz range of the spectra is reproduced. At 50 K we see two pairs of lines with somewhat differing widths and heights. They clearly arise from two magnetically distinguishable, rapidly reorienting CD_3 groups. At 15 K we essentially see the same two pairs of lines but the inner one is split in two barely resolved components and a shoulder. When the temperature is increased, the splitting of the components becomes bigger and the outer pair of lines also starts to develop resolved components. For $T > 30$ K the lines broaden, their separation somehow diminishes and eventually disappears, and they become narrow again.

When we increase the temperature from 15 K on, the first changes in the spectra obviously parallel those which we have simulated in Figure 3. This means that the tunnel frequency decreases on increasing T. In the bottom row of Fig. 10 we show simulations for the central row of the experimental spectra, where the tunnel frequency ν_t has been treated as the only adjustable parameter. The optimal value of ν_t is given together with each simulated spectrum. We think that the match between the experimental and the simulated spectra in Fig. 10 is convincing enough for claiming that we have *measured* the tunnel frequency ν_t in aspirin, and its temperature dependence.

In Fig. 11 we have plotted ν_t versus the temperature. We shall discuss these results and the full curve in Fig. 11 in terms of the hindering potential $V(\varphi)$ in Section 5. Here we focus our attention on another experimental aspect. It concerns a check of our way of inferring ν_t: if it is to make sense, the results must be independent of Υ_{AB}. Therefore we repeated the whole procedure for two more rotation angles of the AB-crystal, $\Upsilon_{AB} = 120°$ and $\Upsilon_{AB} = 150°$. The results of these runs are also shown in Figure 11. They confirm that indeed our procedure leads to tunnel frequencies which are independent of Υ_{AB}. How sensitively the spectra depend on Υ_{AB}, i.e., on the orientation of $\boldsymbol{B}_0$, is demonstrated by the series of spectra in Figure 12. All these spectra were recorded at $T = 29$ K and the shape of all of them can be accounted for by ν_t=1.35 MHz. For some rotation angles, notably $\Upsilon_{AB} = 0°, 30°$ and 150° the key quantity $|\alpha|$ is large and the shape of the spectrum is highly sensitive to the size of ν_t; for others, e.g. $\Upsilon = 90°$, $|\alpha|$ is small and the spectrum

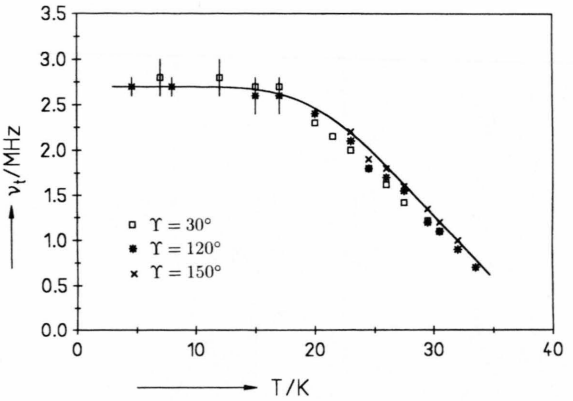

Fig. 11. The temperature dependence of the tunnel frequency ν_t of the CD_3 groups in aspirin. Data are shown for three different rotation angles Υ of the AB-crystal. The full curve is discussed in Section 5. It is a fit of (26) to the experimental data, the fitting parameter being the height V_3 of the potential $V(\varphi)$.

contains no information about ν_t. For $\Upsilon_{AB} = 90°$ the magnetic field $\boldsymbol{B}_0$ lies in the monoclinic plane. As we have stated above, such orientations are not suitable for measuring ν_t.

So far in this subsection, we have discussed the evolution of the $\pm\beta$ lines with increasing temperature. We proceed with considering what happens in this case with the $\pm(|\alpha| \pm \beta)$ and $\pm(2|\alpha| \pm \beta)$ lines. Note that all these lines belong to the E-part of the low-temperature (large ν_t) spectrum.

According to Heuer [10], the pair of E-lines $+|\alpha| - \beta$ and $-|\alpha| - \beta$, for instance, is expected to behave in exactly the same way as the NMR lines of chemically shifted, exchanging protons behave when the exchange rate Ω increases as a result of a rise of the temperature: the lines broaden until they coalesce into a single broad resonance. On further increasing Ω this resonance narrows and eventually becomes a sharp line at the average chemical shift of the two protons. The average position of the $+|\alpha| - \beta$ and $-|\alpha| - \beta$ (and of the $+2|\alpha| - \beta$ and $-2|\alpha| - \beta$) lines is $-\beta$. The average position of the two other pairs of E-lines is $+\beta$. The coalesced narrowed E-lines thus appear at the positions of the lines of the rapidly reorienting CD_3 group which are also the positions of the A-lines and of the $\pm\beta$ pair of E-lines. According to Heuer neither the $\pm\beta$ A-lines nor the $\pm\beta$ E-lines should be affected by a rise of the temperature. The quantity

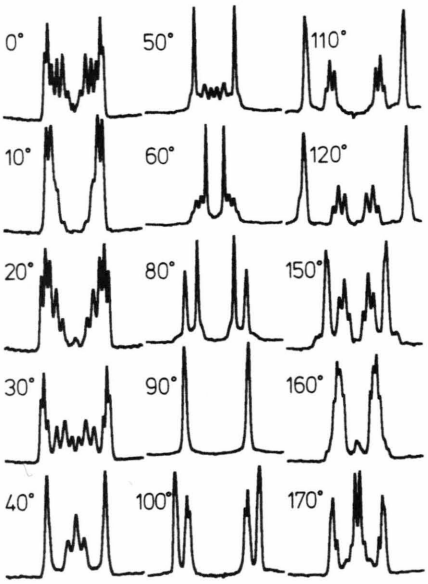

Fig. 12. Temperature T = 29 K: dependence of the shape of the deuteron NMR spectra of the AB-crystal on the rotation angle Υ. All these spectra can well be accounted for by ν_1=1.35 MHz and the known change of orientation of $\boldsymbol{B}_0$ in the molecular axes systems of the two sets of crystallographically equivalent and magnetically inequivalent CD_3 groups in aspirin.

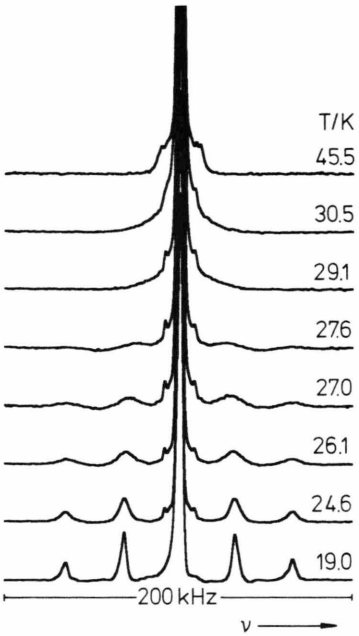

Fig. 13. Temperature dependence of the deuteron spectrum of the B-crystal for the special crystal orientation Υ = 30° where β = 0, see Figure 9. Note the broadening and the (small) shift of the $\pm|\alpha|$ and $\pm 2|\alpha|$ lines for 20 K $\lesssim T \lesssim$ 28 K, and the narrowing of the lorentzian foot in the center of the spectrum for $T \gtrsim$ 29 K. The 27.0 K and 27.6 K spectra are rescaled by a factor of two, the 29.1 ... 45 K spectra by a factor of four. The pedestal with two horns in the center of the spectra is probably due to a small, slightly misaligned piece of the crystal.

of the tunneling methyl group which is analogous to the exchange rate Ω was termed Γ by Heuer. The temperature dependence of Γ is expected to obey the Arrhenius equation, and Heuer thought that the activation energy E_a in this equation can be identified with the energy separation $E^{(1)} - E^{(0)}$ of the first excited and the ground librational levels of the CD_3 group in the potential $V(\varphi)$.

We tested Heuer's theory with the B-crystal at two different rotation angles Υ. On the one hand we selected Υ = 0° because there the $\pm(|\alpha| \pm \beta)$ and $\pm(2|\alpha| \pm \beta)$ lines in the 12.5 K spectrum are particularly "lonesome" and sharp, see bottom spectrum in Figure 8. For this rotation angle we recorded spectra between 11.5 K and 30 K at increments of T of 1.5 K. Another such run (with an extension of the upper temperature to 50 K) we made at Υ = 96°, where β is zero and the spectrum is particularly simple.

From this run we present a selection of spectra in Figure 13. We find indeed, as Heuer predicted, that the width $\delta\nu$ of the E-lines increases with rising temperature. The coalescence temperature is somewhere between 28 K and 29 K. In the spectrum recorded at 29.1 K there is clearly a broad "foot" under the large central line. At 30.5 K this foot has become narrower, and at 45.5 K it has disappeared altogether. We have thus observed not only the predicted broadening of the E-lines but also the narrowing of the coalesced resonance. In the low temperature part of the broadening-coalescing-narrowing process the "exchange" contribution to the linewidth $\delta\nu(T)$ is proportional to Γ. The predicted Arrhenius behaviour of $\Gamma(T)$ must therefore be reflected by $\delta\nu(T) - \delta\nu(T \to 0)$. In Fig. 14 we have plotted our respective data from the Υ = 96° run versus $1/T$. Within experimental error they fall on straight lines, i.e., they follow the Arrhenius equa-

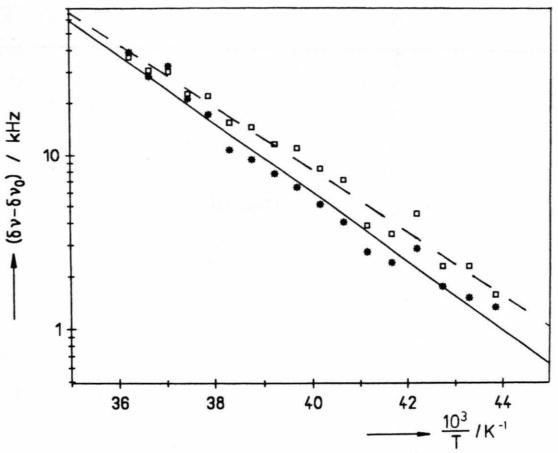

Fig. 14. Arrhenius plot of the temperature dependent contribution $\delta\nu(T) - \delta\nu_0$ to the width $\delta\nu(T)$ of the $\pm|\alpha|$ (stars) and the $\pm 2|\alpha|$ (squares) lines in the spectra of Figure 13. The slopes of the full and dashed straight lines correspond to activation energies of 39.7 meV and 36.0 meV.

tion. The slopes of the straight lines correspond to E_α = 39.7 meV for the $|\alpha|$ and E_a = 36 meV for the $2|\alpha|$ lines. There is a natural reason why the first number is somewhat larger: simulations of spectra (not shown) for the appropriate orientation of B_0, which take into account the temperature dependence of ν_t, show that the $\pm|\alpha|$ lines split in two components with increasing T, while the $\pm 2|\alpha|$ lines remain single. The broadening of the $\pm|\alpha|$ lines thus reflects in part an unresolved splitting while that of the $\pm 2|\alpha|$ is entirely due to a dynamic damping process.

In Sect. 5 we shall inquire whether or not the number for E_a can be identified with $E^{(1)} - E^{(0)}$. As we already hinted in the introduction it actually cannot.

4.4 Temperature dependence of the spin lattice relaxation time T_1

There are two obvious reasons for measuring the temperature dependence of T_1. The first is simply the need of knowing T_1 for adjusting properly the repetition time of the firing of the pulses when spectra are to be recorded. To illustrate this point we mention that for CD_3OH in hydrochinon and methyl-deuterated paraxylene in Dianin's compound T_1 is of the order of 10 hours at the temperature where the methyl group enters the tunneling regime, which happens in these compounds around 12 K. The second reason for measuring T_1 is that its temperature dependence allows, under favourable circumstances, to infer the height V_3 of the hindering potential $V(\varphi)$.

The relaxation rate $1/T_1$ is given by [20]

$$\frac{1}{T_1} = \frac{K_1\tau_c}{1+(\omega_L+\omega_t)^2\tau_c^2} + \frac{K_1\tau_c}{1+(\omega_L-\omega_t)^2\tau_c^2} + \frac{4K_2\tau_c}{1+(2\omega_L+\omega_t)^2\tau_c^2} + \frac{4K_2\tau_c}{1+(2\omega_L-\omega_t)^2\tau_c^2}, \quad (24)$$

where $\omega_t = 2\pi\nu_t$, and τ_c is the correlation time of the reorientations of the CD_3 group, K_1 and K_2 are constants which depend on the orientation of $\boldsymbol{B}_0$. As ν_t = 2.7 MHz is much smaller than the Larmor frequency $\nu_L = \omega_L/2\pi$ = 72.1 MHz, we may simplify (24) and write

$$\frac{1}{T_1} = \frac{2K_1\tau_c}{1+\omega_L^2\tau_c^2} + \frac{8K_2\tau_c}{1+4\omega_L^2\tau_c^2}. \quad (25)$$

With $K_1 = K_2$, which is valid *on the average* for all orientations of $\boldsymbol{B}_0$, equation (25) is just the BPP equation. The temperature dependence of τ_c is expected to follow an Arrhenius equation with an activation energy E_a' which should be a measure of the potential height V_3 (to be precise: V_3 minus the ground state energy $E^{(0)}$).

We have measured $T_1(T)$ of the AB-crystal in the orientation Υ_{AB} = 120° using the saturation-recovery technique. We have evaluated T_1 separately for the two distinguishable methyl groups. The recovery of the magnetization was exponential within experimental errors at all temperatures.

In Fig. 15 we show the results. At ambient temperature both T_1 are about 2.3 s. On lowering the temperature they decrease and go through a minimum at T = 52 K. The slopes of $\log T_1$ vs. $1/T$ are the same to the left and right of the minimum, apart from the sign. The increase of T_1 on the low temperature side starts to level off at about the same temperature where E-lines are first observed in the spectrum ($\approx$ 28 K). The departure of $\log T_1$ from linearity can be explained by assuming that it is governed by an Arrhenius law behaviour with different apparent activation energies in different temperature regimes [15]. In the limit $T \to 0$, it is related to the energy of the first excited librational level, while at higher temperatures transitions to higher librational levels must be taken into account.

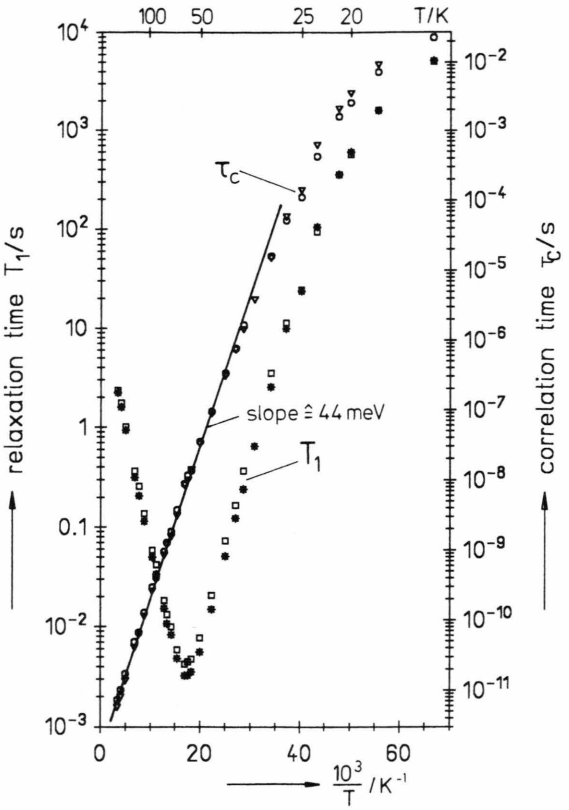

Fig. 15. Temperature dependence of the deuteron spin-lattice relaxation time T_1 of the AB-crystal in the orientation $\Upsilon = 120°$ (cf. Figure 7). The stars (squares) are from the outer (inner) pair of lines. Also shown is the temperature dependence of the correlation time τ_c of the methyl group reorientations calculated from the T_1 data using (25). Note that the τ_c data fall on a straight line over more than five decades.

While the T_1 of the two methyl groups are noticeably different for $T \gtrsim 26$ K they become equal thereafter. The reason for the *difference* is the different orientation of $\boldsymbol{B}_0$ in the molecular axes systems of the two groups. The reason for the *equality* at $T \lesssim 26$ K, where $T_1 > 10$ s, is spin diffusion. Note that the measured T_1 is about 4000 s at $T = 15$ K.

We now inquire about the temperature dependence of τ_c and about E_a'. For the sake of simplicity we assume $K_1 = K_2 =: K$. This assumption is not critical but is convenient since it allows solving (25) for τ_c when T_1 is known, i.e., has been measured. The required value of K can be found from the minimum of T_1 which occurs when $\omega_L \tau_c = 0.615$. It is given by $K = 0.702 \cdot \omega_L / T_1$ (min).

The temperature dependence of τ_c obtained in this way from our $T_1(T)$ data is also shown in Figure 15. The slope of $\log \tau_c$ vs. $1/T$ is constant over more than five decades of τ_c and corresponds to $E_a' = (44 \pm 0.5)$ meV. In the concluding section we shall compare this value with V_3 derived from the limiting low-temperature value of ν_t.

5. Conclusions

The most important result of this work is that we have been able to record spectra which closely match those predicted theoretically for CD_3 groups. The match is, however, not perfect. As mentioned in Sect. 4.2, the splitting of the pairs of E-lines in the 12.5 K spectra of the B crystal is consistently smaller by roughly 1 kHz (which is less than the linewidth, but nevertheless *real*) than the splitting 2β of the A-lines. In addition the predicted 1:2:12 ratios of the line intensities could not be verified quantitatively, and again we feel that the blame for the discrepancy cannot be put on the quality of the spectra. This means that there is a need for refining the theory which so far is based on a number of simplifying assumptions, the most critical ones being probably those of a *rigid* rotor and *exact* C_3 symmetry.

We now turn to our observations which relate to the hindering potential $V(\varphi)$. The first is the tunnel frequency in the limiting case $T \to 0$. The number we obtained for this quantity is 2.7 MHz with an estimated error of not more than ± 0.1 MHz. With the Mathieu equation as the link it enables us to infer the height V_3 of $V(\varphi)$. The number we get is $V_3 = (47.2 \pm 0.5)$ meV. The *assumption* on which this conclusion rests is that $V(\varphi)$ is purely threefold, i.e., given by (6).

The second observation related to $V(\varphi)$ is the temperature dependence of ν_t. The observed decrease of ν_t for $T \gtrsim 17$ K does not mean, of course, that the height of the potential decreases. It rather reflects the fact that the ensemble of CD_3 groups in our crystal no longer occupies exclusively the librational ground level. To account for the temperature dependence of the observable tunnel frequency it is natural to make the following assumptions: (i) The various librational levels are occupied according to the Boltzmann distribution. (ii) Phonon driven transitions between the librational levels are restricted to the ladder of the

$|nA\rangle$ on the one, and to that of the $|nE^a\rangle$, $|nE^b\rangle$ states on the other hand. Transitions from $|nA\rangle$ to a $|n'E^{a,b}\rangle$ states virtually do not occur. (iii) The lifetime of a CD_3 group in any of the $|nA\rangle$ or $|nE^{a,b}\rangle$ states is short on the NMR timescale, except for the ground states $|0A\rangle$ and $|0E^{a,b}\rangle$.

These assumptions lead for the temperature dependence of ν_t [21] to:

$$\nu_t(T) = \frac{\sum \Delta_n \cdot \exp(-E^{(n)}/kT)}{h \sum \exp(-E^{(n)}/kT)}. \tag{26}$$

Both summations are over $n = 0, \ldots, \infty$. $E^{(n)}$ is the weighted average of $E_A^{(n)}$ and $E_{E^a,E^b}^{(n)}$. Equation (26) predicts a *decrease* of ν_t with *increasing* temperature because Δ_n is positive for n even while the reverse is true for n odd. Note that $|\Delta_n|$ increases rapidly with increasing n, nevertheless the Boltzmann factors make sure that for reasonably low temperatures the summations in (26) can be limited to only a few terms.

The full curve in Fig. 12 has been calculated from (26). We have again stipulated a purely threefold potential $V(\varphi)$, therefore all the $E^{(n)}$ and Δ_n are fixed by the value of ν_t for $T \to 0$. Except for this value there is no adjustable parameter. The agreement with the experimental data is impressive. The remaining (small) systematic deviations are indicative of a (small) error in the calibration of the thermometer. As the agreement hinges on the stipulation of a purely threefold potential, it may be taken as an argument that the potential $V(\varphi)$ of the CD_3 group in aspirin is very little contaminated by sixfold, ninefold etc. contributions $V_6 \cos(6\varphi + \delta_6)$, $V_9 \cos(9\varphi + \delta_9)$ etc. where δ_6, δ_9 etc. are (unknown) phases.

This conclusion is strengthened by the value of E_a' which we obtained from the relaxation data. Theorists think that E_a' should be identified with the height of the potential *above* the ground state level which is, for a purely threefold potential, equal to $V_3 - E^{(0)}$ [15]. For $V_3 = 47.2$ meV the solution of the Mathieu equation gives $E^{(0)} = 5.7$ meV, which leads for E_a' to the prediction $V_3 - E^{(0)} = 41.5$ meV. This number comes remarkably close to the directly and independently *measured* value, which is 44 meV, and thus confirms the implications of the relaxation theory.

The fourth observation related to $V(\varphi)$ is the activation energy E_a which governs the broadening of the E-lines, cf. Figs. 13 and 14. Heuer expected that this energy should correspond to the energy difference between the first excited and the ground librational level. For $V_3 = 47.2$ meV this difference amounts to 11 meV. The experimental number of 36 meV we got for the $2|\alpha|$-lines is much larger. It suggests that in essence it is also the potential height minus $E^{(0)}$ which governs the broadening of the E-lines. Heuer's theory must obviously be extended by taking into account higher torsional levels. Such an extension should also account for the temperature-dependent widths of the β lines, or their substructures, which can be observed in the top row of Figure 10.

We close by pointing out that the fact that we could analyse and correlate four independent observations all related to $V(\varphi)$ gave us an unusually clear and reliable insight into the size and shape of this hindering potential of the CD_3 group in aspirin. We stress again that the periodicity $V(\varphi) = V(\varphi \pm 120°)$ is a consequence of the permutation symmetry of the deuterons while the physical potential set up by the surroundings of the methyl group in aspirin has no symmetry whatsoever. Currently we explore this physical potential with measurements on aspirin-CDH_2 and hope to be eventually able to correlate it with the periodic, almost purely threefold potential sensed by the fully deuterated methyl group in aspirin.

Acknowledgements

B. Manz and A. Birczyński were involved in the early stage of this work. We gratefully acknowledge their contributions. Z. T. L. and Z. O. appreciate hospitality of the MPI in Heidelberg and acknowledge financial support from the EC grant no. CIPA–CT92. Z. T. L. was also supported by the State Committee for Scientific Research (Poland) grant no. 203649101 during work on this project.

[1] S. Idziak, U. Haeberlen, and H. Zimmermann, Mol. Phys. **73**, 571 (1991).
[2] Z. T. Lalowicz, Ulrike Werner, and W. Müller-Warmuth, Z. Naturforsch. **43a**, 219 (1988).
[3] E. Rössler, M. Taupitz, and H. M. Vieth, Ber. Bunsengesellschaft **93**, 1241 (1989).
[4] K. Börner, G. Diezemann, E. Rössler, and H. M. Vieth, Chem. Phys. Lett. **181**, 563 (1991).
[5] T. Bernhard and U. Haeberlen, Chem. Phys. Lett. **186**, 307 (1991).
[6] B. Manz, Diploma Thesis, University of Heidelberg (1992).
[7] A. C. Hewson, J. Phys. C: Solid State Phys. **15**, 3841, 3855 (1982).
[8] A. Würger, Z. Phys. B - Cond. Matter **76**, 65 (1989).
[9] G. Diezemann, H. Sillescu, and D. van der Putten, Z. Phys. B - Cond. Matter **83**, 245 (1991).
[10] A. Heuer, Z. Phys. B - Cond. Matter **88**, 39 (1992).
[11] J. Freed, J. Chem. Phys. **43**, 1710 (1965).
[12] W. Press, Single Particle Rotations in Molecular Crystals; Springer, Berlin 1981.
[13] T. Bernhard, Ph.D. Thesis, University of Heidelberg (1988).
[14] Ulrike Werner and W. Müller-Warmuth, Z. Phys. B - Cond. Matter **91**, 65 (1993).
[15] D. van der Putten, G. Diezemann, F. Fujara, K. Hartmann, and H. Sillescu, J. Chem. Phys. **96**, 1 (1992).
[16] D. Cavagnat, S. Clough, and F. Zelaya, J. Phys. C: Solid State Phys. **18**, 6457 (1985).
[17] P. J. Wheatley, J. Chem. Soc.**1964**, 6036.
[18] Jadwiga Tritt-Goc, N. Piślewski, and U. Haeberlen, Chemical Physics **102**, 133 (1986).
[19] M. P. Summers, J. E. Carless, and R. P. Enever, J. Pharm. Pharmac. **22**, 615 (1970).
[20] J. Haupt, Z. Naturforsch. **26a**, 1578 (1971).
[21] C. Johnson and C. Mottley, Chem. Phys. Lett. **22**, 430 (1973).

Verantwortlich für den Inhalt: A. KLEMM
Satz und Druck: Konrad Triltsch, Würzburg